Neoclassical Parallel Momentum Balance and Flow Damping in Stellarators

D.A. Spong
Oak Ridge National Laboratory

Acknowledgements: Steve Hirshman, Jim Lyon, Lee Berry, Dave Mikkelsen

2004 Kinetic Theory in Stellarators
Graz, Austria, September 13-15, 2004

Motivations for viscosity/moments based transport analysis

- S. Hirshman, Phys. Fluids **21** (1978) 224.
- S. Hirshman, D. Sigmar, Nuclear Fusion **21** (1981) 1079.
- M. Taguchi, Phys. Fluids B **4** (1992) 3638.
- H. Sugama and S. Nishimura, Physics of Plasmas, **9 (**November, 2002) 4637
- Uses ℓ = 2 Legendre component of f rather than ℓ = 0,1
  - Less affected by neglect of field particle collsions on test particle distribution (test particle component is dominant)
- Momentum conservation is taken into account through fluid momentum balance equations and friction-flow relations
- Multiple species can be more readily decoupled
  - Facilitates development of self-consistent impurity models

Moments Method for Stellarator Transport

- QPS/NCSX/HSX/W7-X have been strongly optimized so that neoclassical losses << anomalous losses
  - The remaining transport-related differences will be in the parallel momentum transport properties
- Recently, a theoretical framework has been developed that allows quantitative, self-consistent assessment of the parallel and perpendicular transport in 3D systems:
  - H. Sugama and S. Nishimura, Physics of Plasmas, **9 (**November, 2002) 4637.
  - Extends DKES transport coefficients (based on pitch-angle scattering operator) to include momentum-conservation and ion-electron frictional coupling effects.
  - Provides particle/energy fluxes, viscosity tensor, flows, and bootstrap current
- This motivates development of a stellarator analog of the NCLASS code
- Calculation of flow velocity profiles for stellarators is motivated by:
  - Relevance to turbulence suppression/enhanced confinement regimes
  - Comparison with impurity line measurements
  - Impurity accumulation/shielding studies
- More accurate collisional bootstrap current prediction, and ambipolar electric field estimation

Moments Method Equations for Stellarators

Parallel momentum balance relations

$$\left\langle \vec{B}\cdot\left(\vec{\nabla}\cdot\vec{\Pi}_a\right)\right\rangle - n_a e_a \langle BE_\parallel \rangle = \langle BF_{\parallel a1}\rangle$$

$$\left\langle \vec{B}\cdot\left(\vec{\nabla}\cdot\vec{\Theta}_a\right)\right\rangle = \langle BF_{\parallel a2}\rangle$$

Friction-flow relations

[S. Hirshman, D. J. Sigmar, Nuclear Fusion **21**, 1079 (1981)]

$$\begin{bmatrix} \langle BF_{\parallel a1}\rangle \\ \langle BF_{\parallel a2}\rangle \end{bmatrix} = \sum_b \begin{bmatrix} l_{11}^{ab} & -l_{12}^{ab} \\ -l_{12}^{ab} & l_{22}^{ab} \end{bmatrix} \begin{bmatrix} \langle Bu_{\parallel b}\rangle \\ \frac{2}{5p_b}\langle Bq_{\parallel b}\rangle \end{bmatrix}$$

The viscous stress tensor components and flows have been related to DKES transport coefficients by H. Sugama, S. Nishimura, Phys. Plasmas 9, 4637 (2002):

$$\begin{bmatrix} \left\langle \vec{B}\cdot\left(\vec{\nabla}\cdot\vec{\Pi}_a\right)\right\rangle \\ \left\langle \vec{B}\cdot\left(\vec{\nabla}\cdot\vec{\Theta}_a\right)\right\rangle \\ \Gamma_a \\ Q_a/T_a \end{bmatrix} = \begin{bmatrix} M_{a1} & M_{a2} & N_{a1} & N_{a2} \\ M_{a2} & M_{a3} & N_{a2} & N_{a3} \\ N_{a1} & N_{a2} & L_{a1} & L_{a2} \\ N_{a2} & N_{a3} & L_{a2} & L_{a3} \end{bmatrix} \begin{bmatrix} \langle u_{\parallel a}B\rangle/\langle B^2\rangle \\ \frac{2}{5p_a}\langle q_{\parallel a}B\rangle/\langle B^2\rangle \\ X_{a1} \\ X_{a2} \end{bmatrix}$$

where $\left[M_{aj}, N_{aj}, L_{aj}\right] = n_a \frac{2}{\sqrt{\pi}} \int_0^\infty dK \sqrt{K} e^{-K} \left(K - \frac{5}{2}\right)^{j-1} \left[M_a(K), N_a(K), L_a(K)\right]$

$$M_a(K) = \frac{m_a^2}{T_a}\left[v_D^a(K)\right]^2 D_{33}(K)\left[1 - \frac{3m_a v_D^a(K) D_{33}(K)}{2T_a K\langle B^2\rangle}\right]^{-1}$$

$$N_a(K) = \frac{m_a}{T_a} v_D^a(K) D_{13}(K)\left[1 - \frac{3m_a v_D^a(K) D_{33}(K)}{2T_a K\langle B^2\rangle}\right]^{-1}$$

$$L_a(K) = \frac{1}{T_a}\left\{ D_{11}(K) - \frac{B^2 v^2 v_D^a}{3\Omega_a^2}\langle \tilde{U}^2\rangle \right\}$$

$$+ \frac{3m_a v_D^a(K)\left[D_{13}(K)\right]^2}{2T_a^2 K\langle B^2\rangle}\left[1 - \frac{3m_a v_D^a(K) D_{33}(K)}{2T_a K\langle B^2\rangle}\right]^{-1}$$

D_{11}

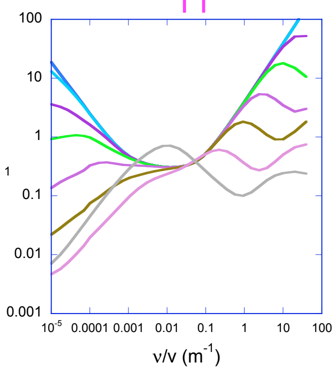

D_{13}

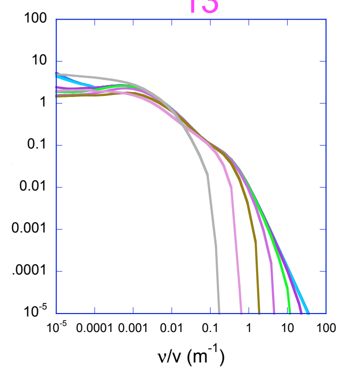

D_{33}

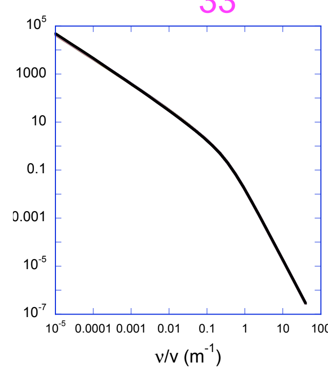

Radial fluxes, bootstrap current, and parallel, poloidal, toroidal flow velocities are obtained via the parallel force balance relation:

Radial particle flows required for ambipolar condition ⇨ self-consistent energy fluxes and bootstrap currents

$$\begin{bmatrix} \Gamma_e \\ q_e/T_e \\ \Gamma_i \\ q_i/T_i \\ J_{BS}^E \end{bmatrix} = \begin{bmatrix} L_{11}^{ee} & L_{12}^{ee} & L_{11}^{ei} & L_{12}^{ei} & L_{1E}^{e} \\ L_{21}^{ee} & L_{22}^{ee} & L_{21}^{ei} & L_{22}^{ei} & L_{2E}^{e} \\ L_{11}^{ie} & L_{12}^{ie} & L_{11}^{ii} & L_{12}^{ii} & L_{1E}^{i} \\ L_{21}^{ie} & L_{22}^{ie} & L_{21}^{ii} & L_{22}^{ii} & L_{2E}^{i} \\ L_{E1}^{e} & L_{E2}^{e} & L_{E1}^{i} & L_{E2}^{i} & L_{EE} \end{bmatrix} \begin{bmatrix} X_{e1} \\ X_{e2} \\ X_{i1} \\ X_{i2} \\ X_E \end{bmatrix} \quad \text{where } X_{a1} \equiv -\frac{1}{n_a}\frac{\partial p_a}{\partial s} - e_a\frac{\partial \Phi}{\partial s},\ X_{a2} \equiv -\frac{\partial T_a}{\partial s},\ X_E = \langle BE_\parallel \rangle / \langle B^2 \rangle^{1/2}$$

Parallel mass and energy flows:

$$\begin{bmatrix} \langle Bu_{\parallel i} \rangle \\ \frac{2}{5p_i}\langle Bq_{\parallel i} \rangle \end{bmatrix} = \left[\frac{1}{\langle B^2 \rangle} \begin{bmatrix} M_{i1} & M_{i2} \\ M_{i2} & M_{i3} \end{bmatrix} - \begin{bmatrix} l_{11}^{ii} & -l_{12}^{ii} \\ -l_{12}^{ii} & l_{22}^{ii} \end{bmatrix} \right]^{-1} \begin{bmatrix} N_{i1} & N_{i2} \\ N_{i2} & N_{i3} \end{bmatrix} \begin{bmatrix} X_{i1} \\ X_{i2} \end{bmatrix}$$

Poloidal and toroidal (contra-variant) flow velocities:

$$\begin{bmatrix} \langle \mathrm{u}_\mathrm{i}^\theta \rangle / \chi' \\ \langle \mathrm{u}_\mathrm{i}^\zeta \rangle / \psi' \end{bmatrix} = \frac{4\pi^2}{V'} \begin{bmatrix} 1 & -B_\zeta / \left(\chi' \langle B^2 \rangle\right) \\ 1 & B_\theta / \left(\psi' \langle B^2 \rangle\right) \end{bmatrix} \begin{bmatrix} \langle Bu_{\parallel i} \rangle / \langle B^2 \rangle \\ X_{i1} \end{bmatrix}$$

Parallel Environment for Neoclassical Transport Analysis (PENTA)

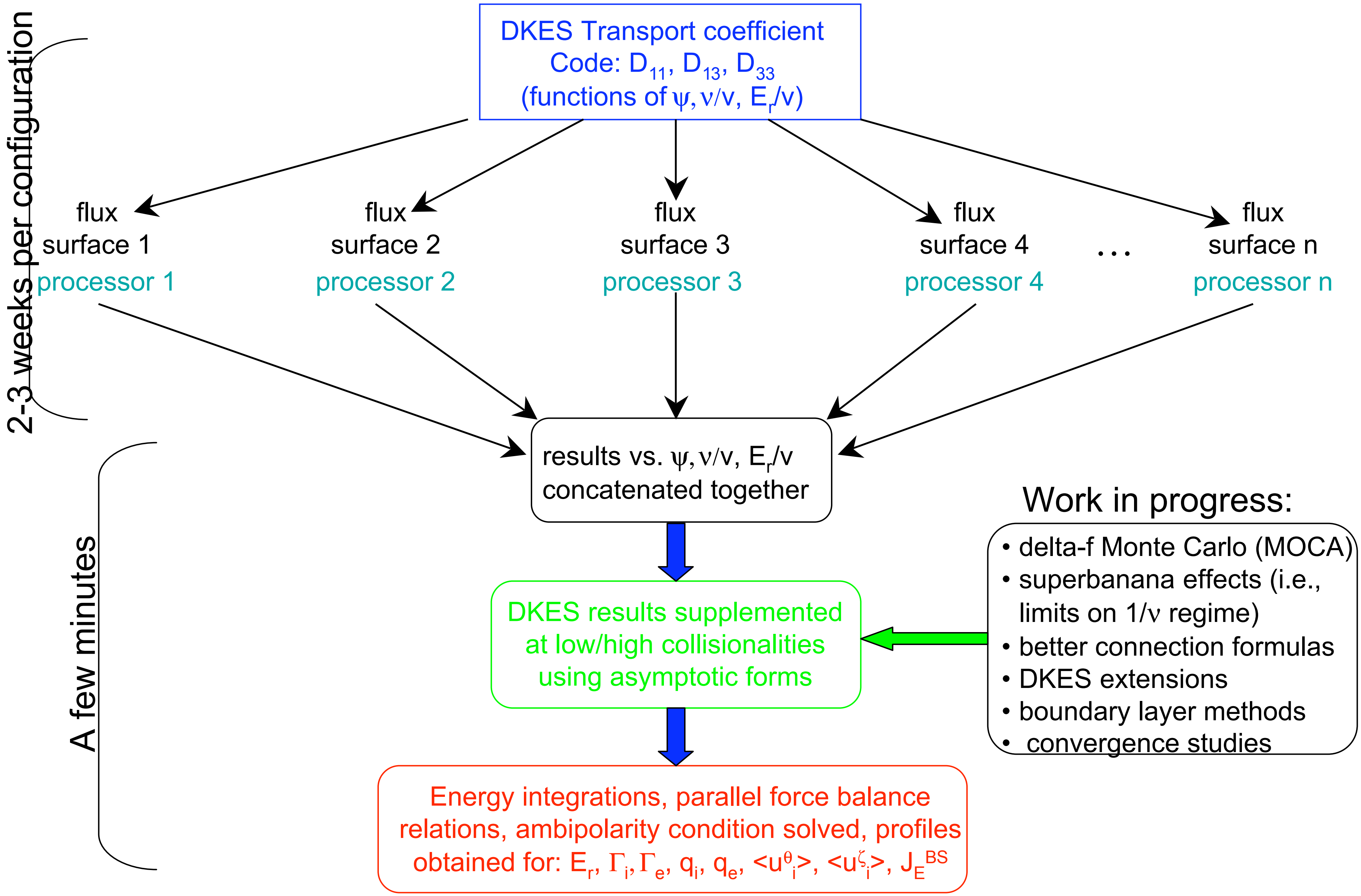

In addition to the usual three DKES coefficients the flux surface averaged Pfirsch-Schlüter flow U is required

$$\vec{v}=\frac{1}{eB}\left(-\frac{1}{n}\frac{\partial p}{\partial\psi}-e\frac{\partial\Phi}{\partial\psi}\right)\vec{\nabla}\psi\times\frac{\vec{B}}{B}$$

$$+\left[\frac{\langle u_{\parallel}B\rangle}{\langle B^{2}\rangle}+\frac{1}{eB}\left(-\frac{1}{n}\frac{\partial p}{\partial\psi}-e\frac{\partial\Phi}{\partial\psi}\right)\tilde{U}\right]\frac{\vec{B}}{B}$$

In order for $\vec{v}$ to maintain incompressibility,

$\tilde{U}$ must satisfy:

$$\vec{B}\cdot\vec{\nabla}\left(\frac{\tilde{U}}{B}\right)=\vec{B}\times\vec{\nabla}\psi\cdot\vec{\nabla}\left(\frac{1}{B^{2}}\right)$$

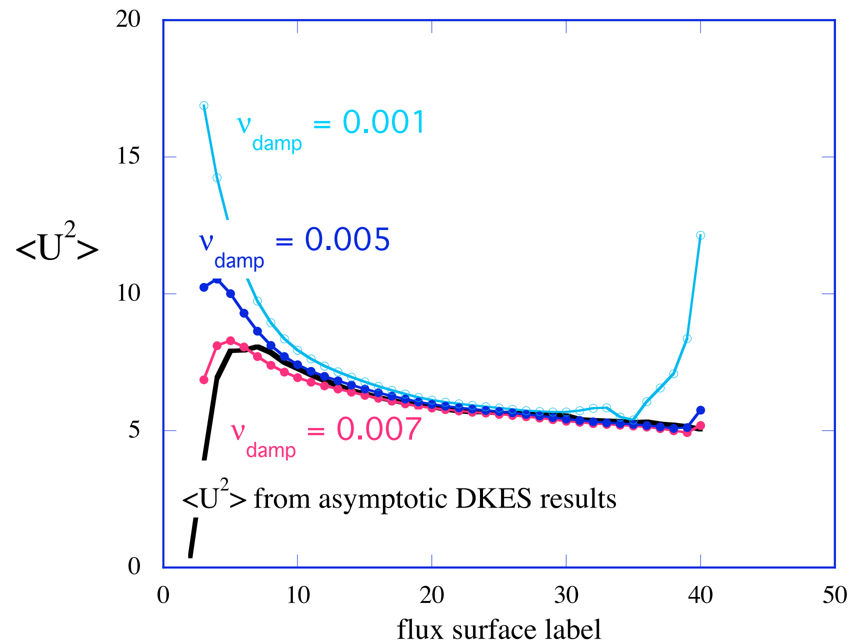

$\langle U^2\rangle$ can be obtained by:

-solving this equation directly (with damping to resolve singularities at rational surfaces)

- matching to high collisionality DKES coefficient: $\langle U^2\rangle = 1.5L_{11}v/\nu$ (for large v/ν

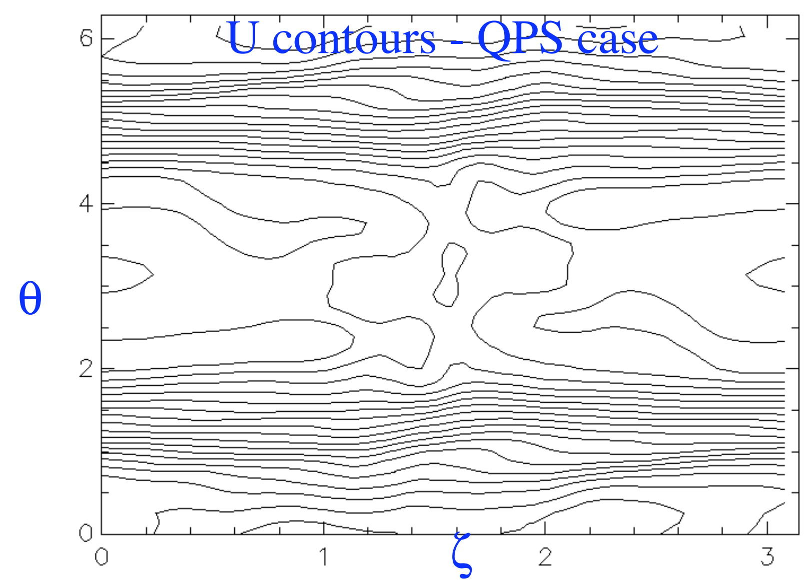

Direct calculation of U is useful for:

- obtaining non-averaged flow velocity
- calculating other components than provided in the Sugama, Nishimura paper
- flow visualization/comparison with expt.

Current approach: DKES data base + analysis/physics based extensions

- Within the data base, ln(M), ln(N), ln(L) vs. ln(ν/v) and ln(E/v) are interpolated using 2-d splines
- Goal
  - use testing to determine regimes insensitive to form of extension
  - Improve extensions as better methods become available
- Examples
  - Low collisionality D_{11}
    - $D_{11} \propto 1/\nu$ for plateau $> \nu > E_s$
    - $D_{11} \propto \nu$ for $\nu < E_s$
    - $D_{11} \propto \nu^{1/2}$ for transition region
  - Low collisionality D_{31}
    - Match to lowest D_{31} from DKES then constant at lower collisionality
  - High collisionality, high electric field
    - Incompressibility assumption breaks down
    - Viscosities can go negative or develop unphysical scalings with ν
    - Merge into E_s = 0 result for $\nu > \nu_{critical}$

Upper/lower bound convergence tests

High density ICH regime (errors neglible)

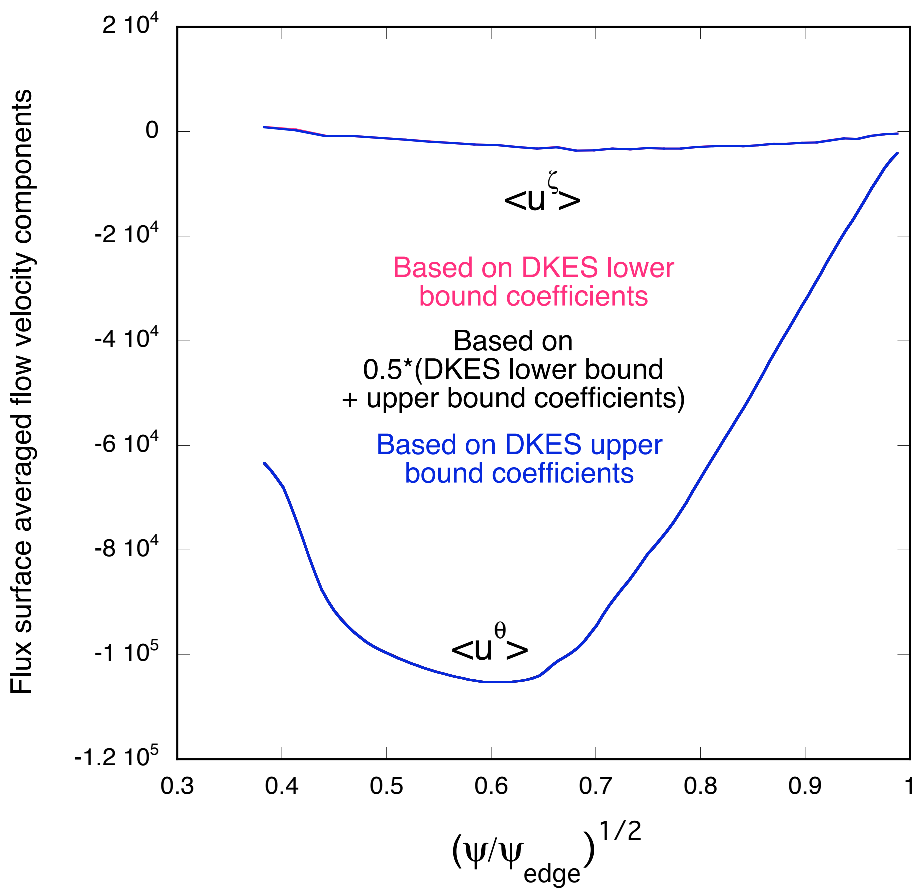

Low density ECH regime (errors < 25%)

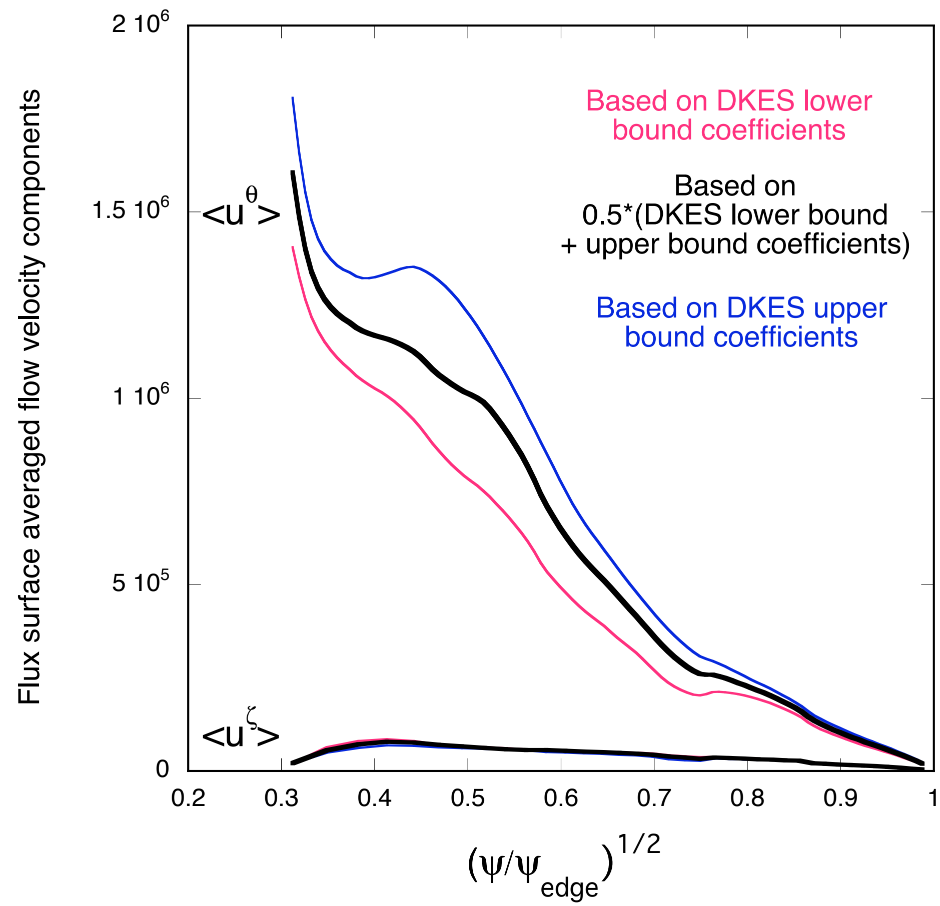

Energy integrations (adaptive) are monitored:

footprint of accesses in collisionality/electric field

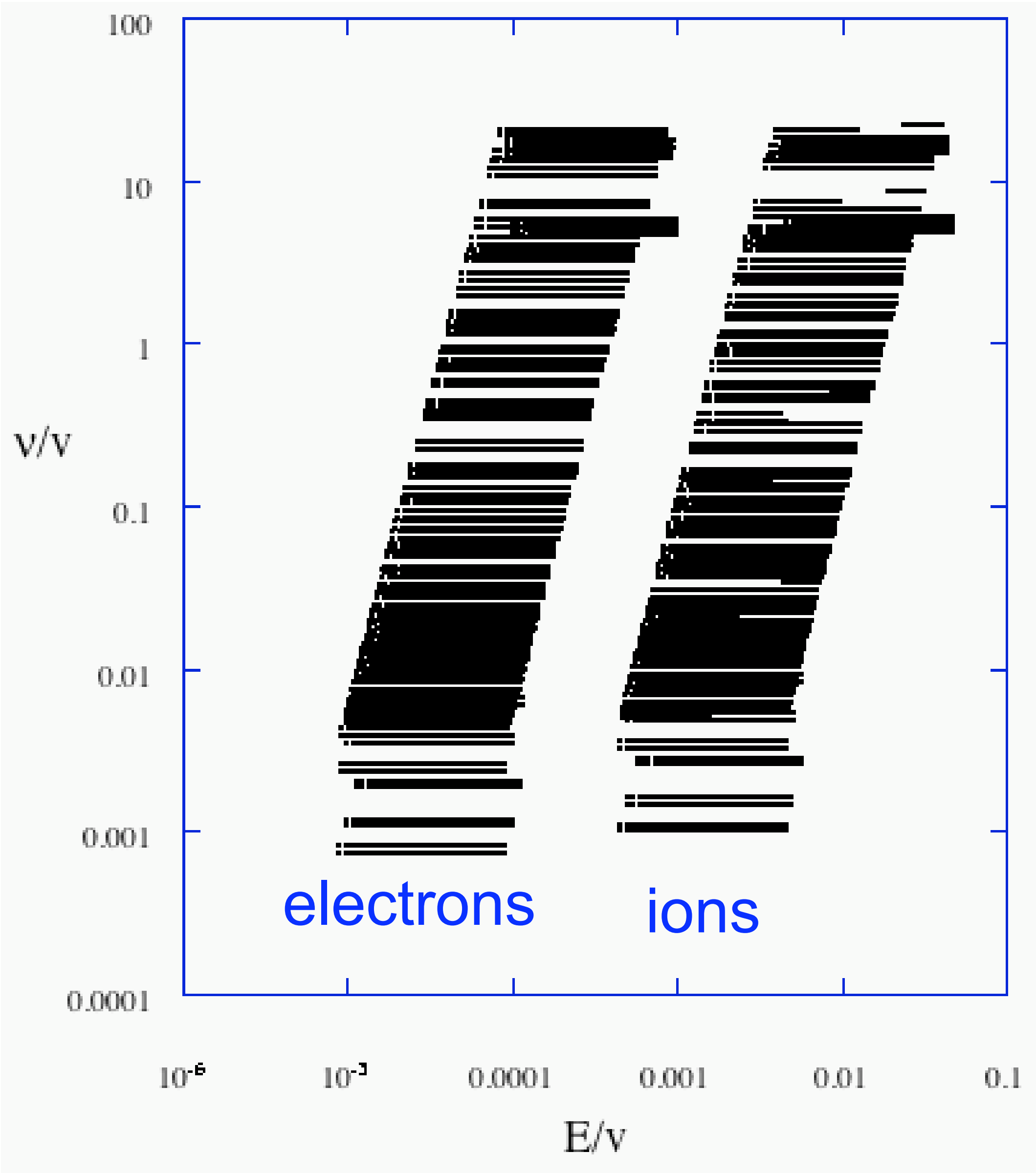

Quasi-symmetric stellarators based on the three forms of quasi-symmetry are now either operational or planned within the U.S. fusion program

- HSX: quasi-helical symmetry $|B| \sim |B|(m\theta - n\zeta)$; NCSX: quasi-toroidal symmetry $|B| \sim |B|(\theta)$; QPS: quasi-poloidal symmetry $|B| \sim |B|(\zeta)$
- This analysis has also been verified for the tokamak (indicating $\Gamma_{ion} = \Gamma_{elec}$ at $E_r = 0$)

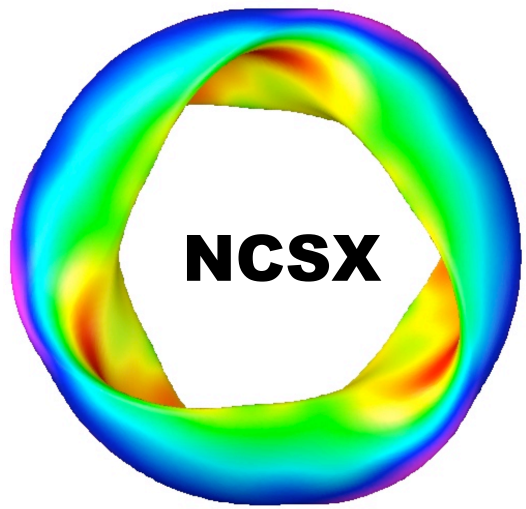

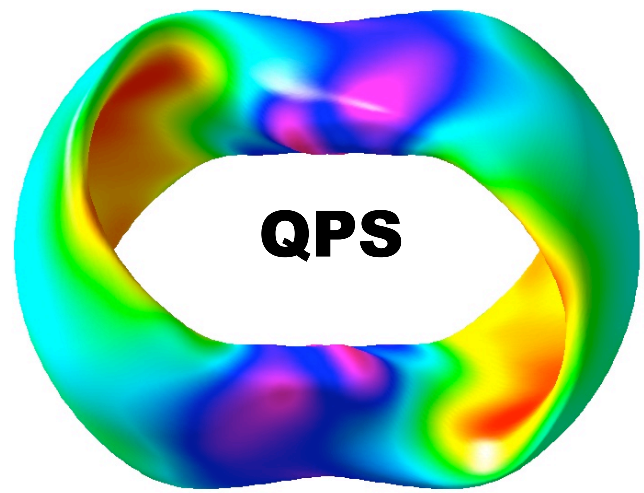

Univ. of Wisconsin

Princeton Plasma Physics Lab.

Oak Ridge National Lab.

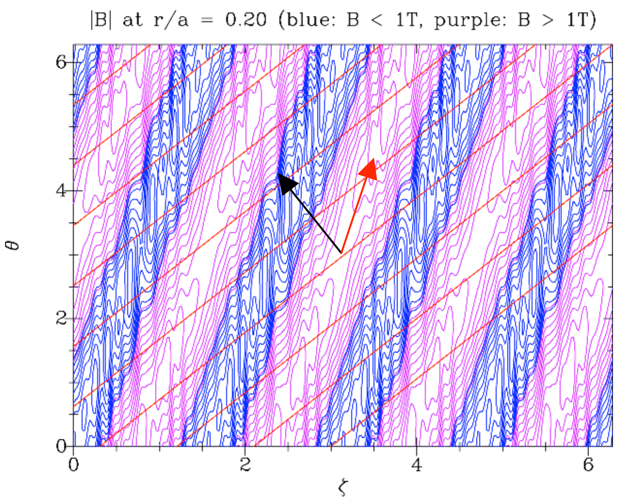

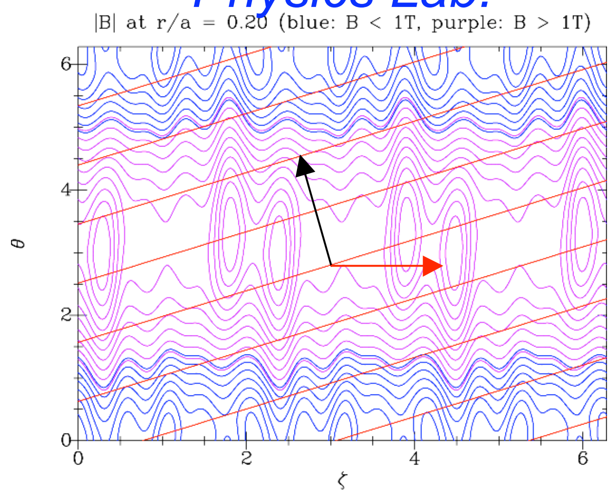

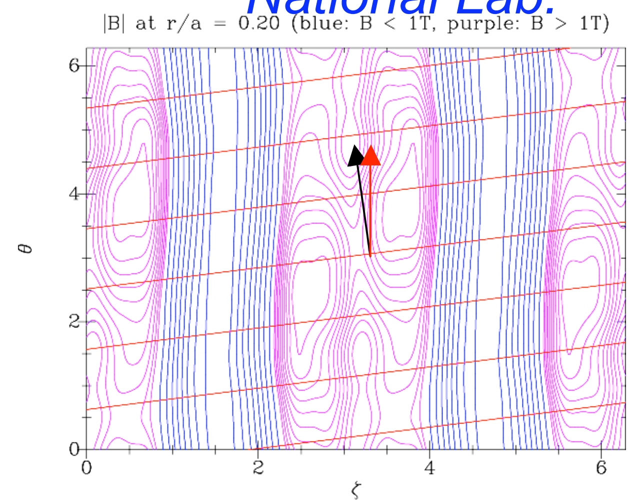

Profiles and parameters

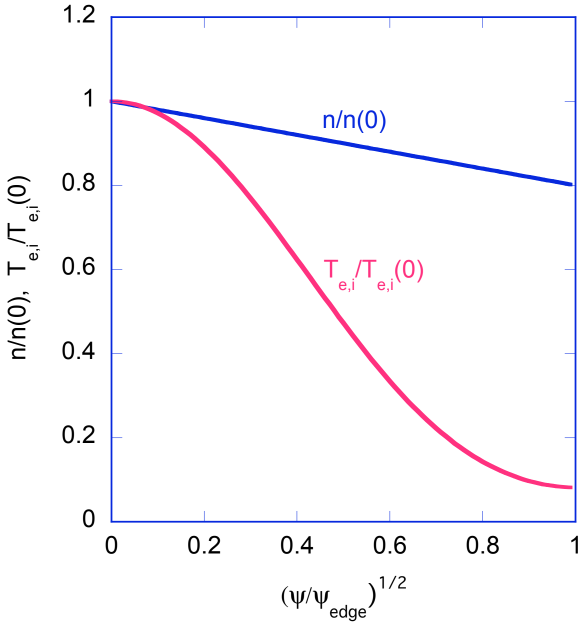

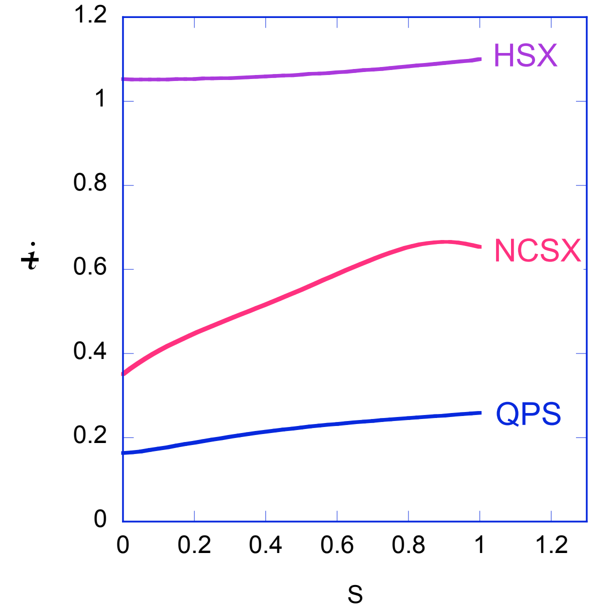

ECH Regime:

$n(0) = 2 \times 10^{19}\ m^{-3}$
$T_e(0) = 2.1$ keV
$T_i(0) = 0.2$ keV

ICH Regime:

$n(0) = 8.3 \times 10^{19}\ m^{-3}$
$T_e(0) = 0.53$ keV
$T_i(0) = 0.38$ keV

Typical QPS DKES monoenergetic transport coefficients

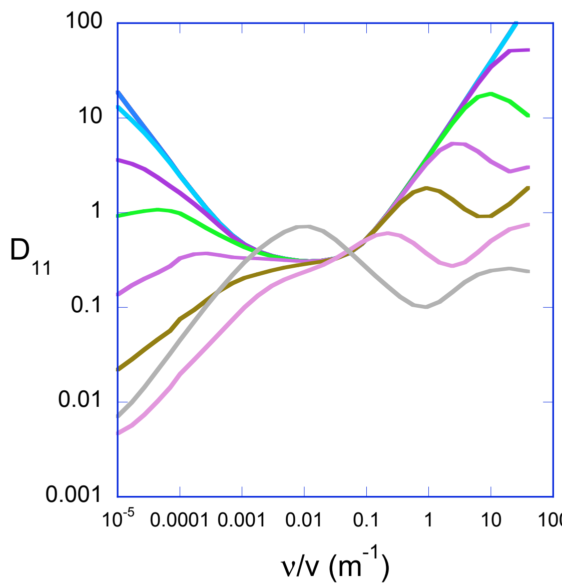

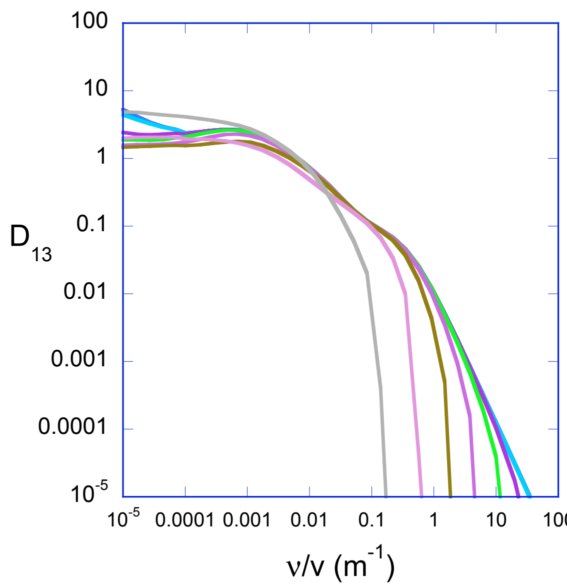

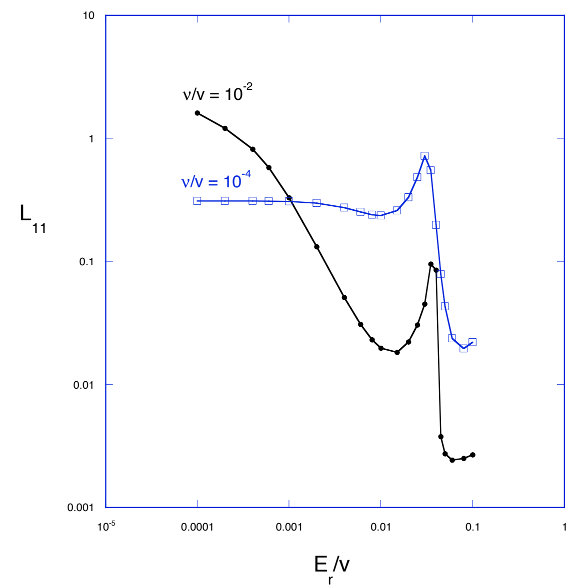

QPS - viscosities show strongly reduced poloidal flow damping from an equivalent axisymmetric device

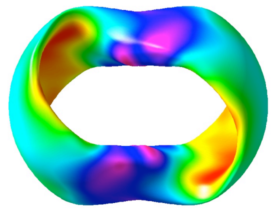

poloidal - 10 x less than tokamak

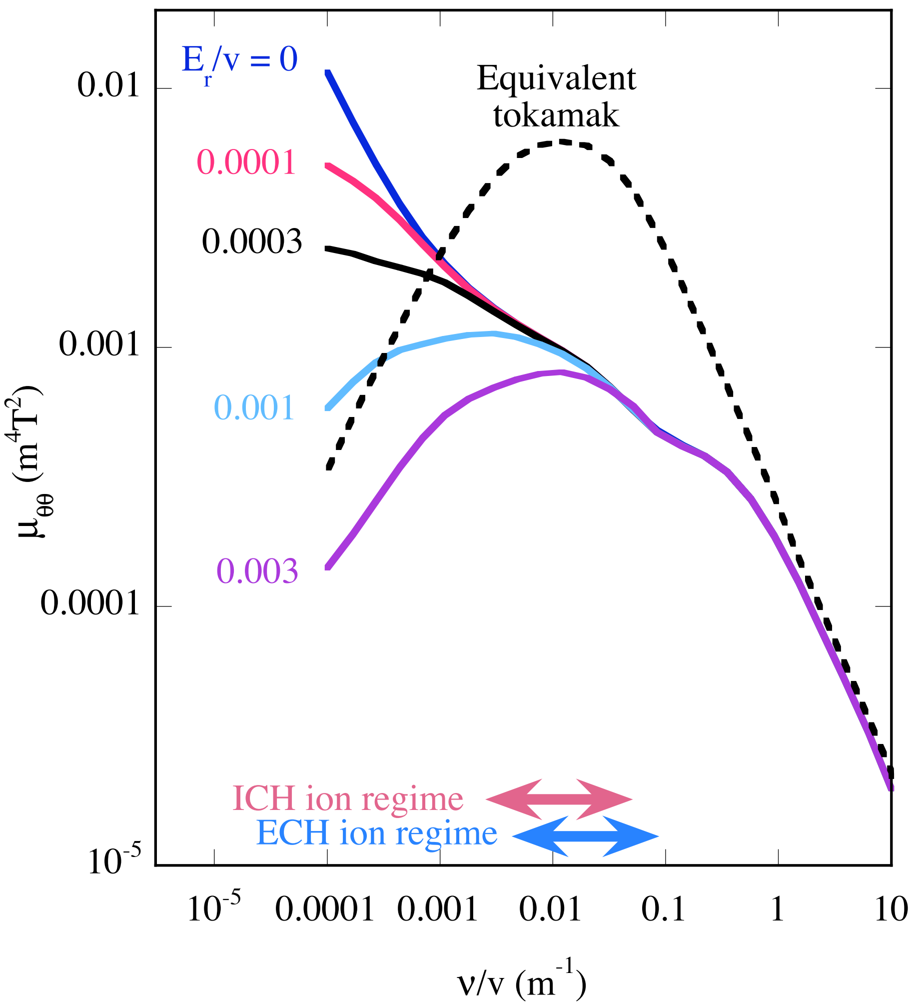

parallel

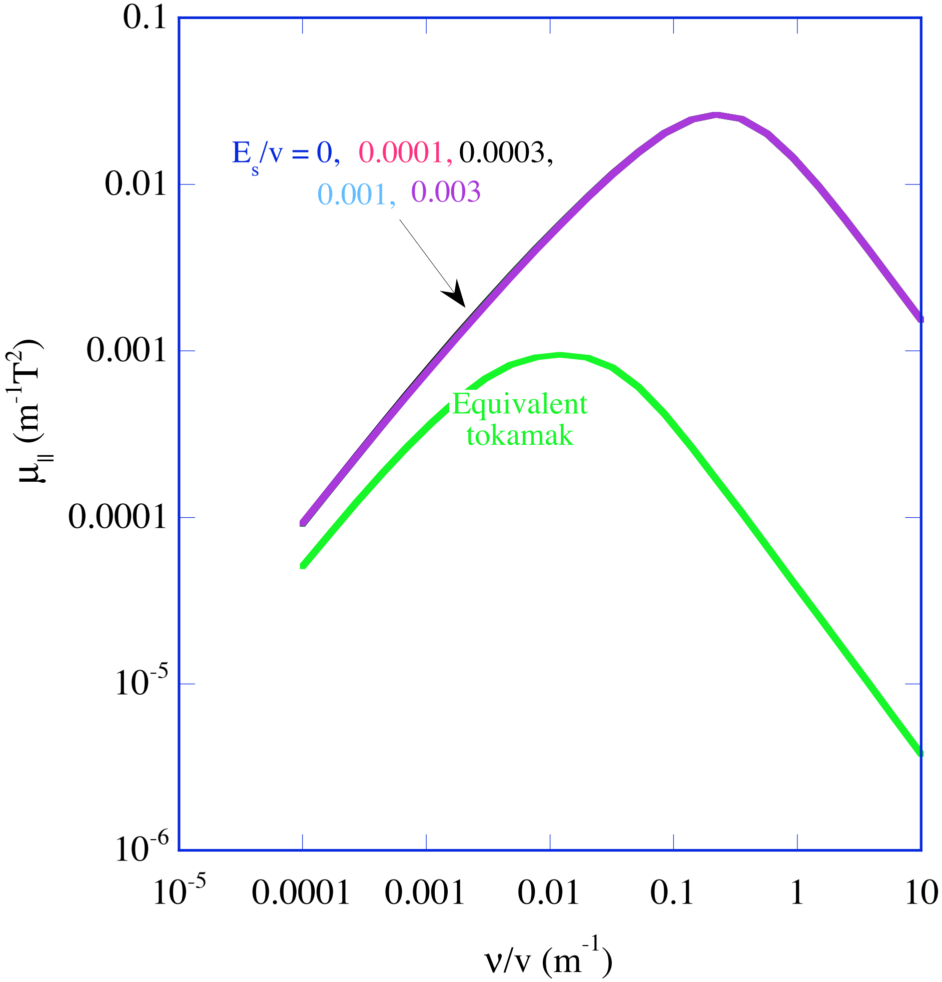

QPS ICH regime has an ion root over the full radius

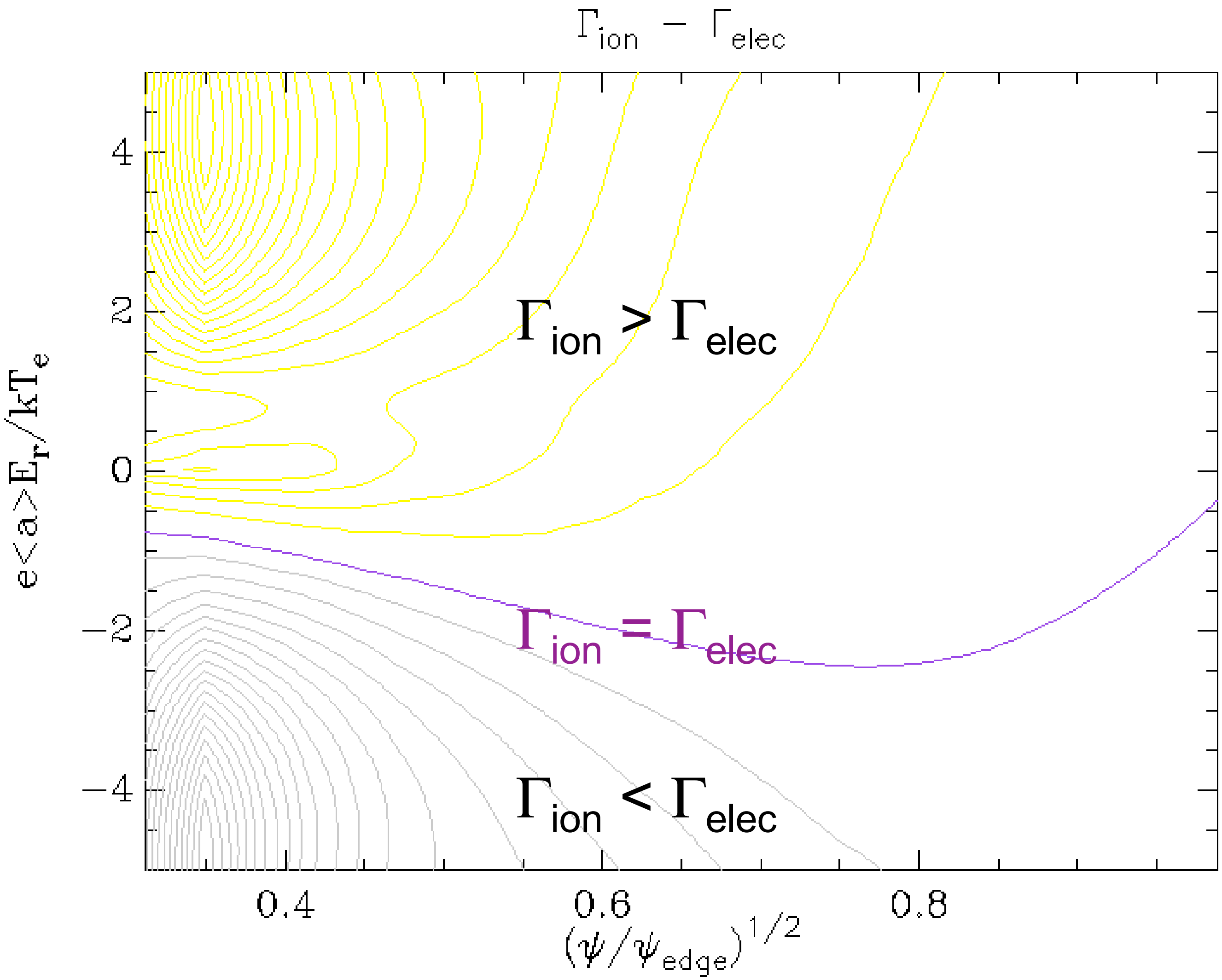

QPS - ICH regime

electric field and flow velocities

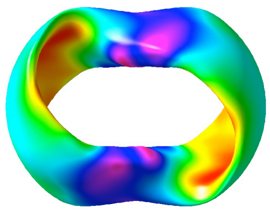

Toroidal flow suppressed - poloidal flow dominates

$n(0) = 8.3 \times 10^{19}\ m^{-3}$, $T_e(0) = 0.53$ keV, $T_i(0) = 0.38$ keV

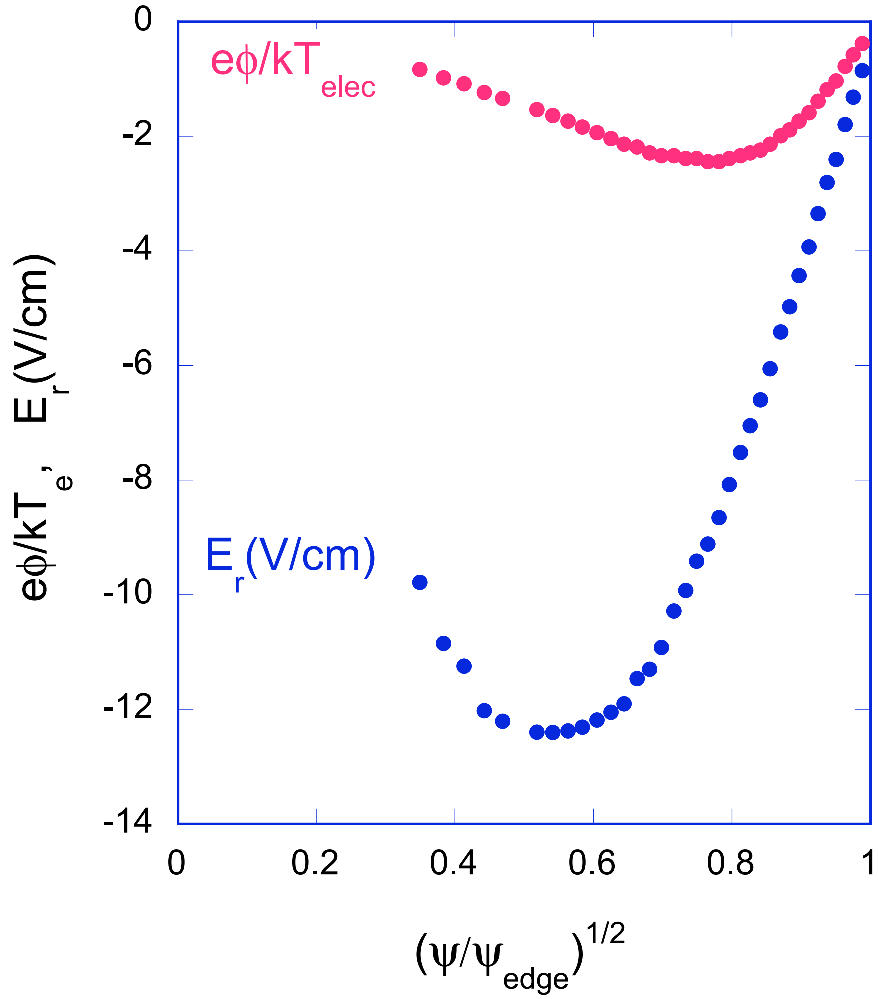

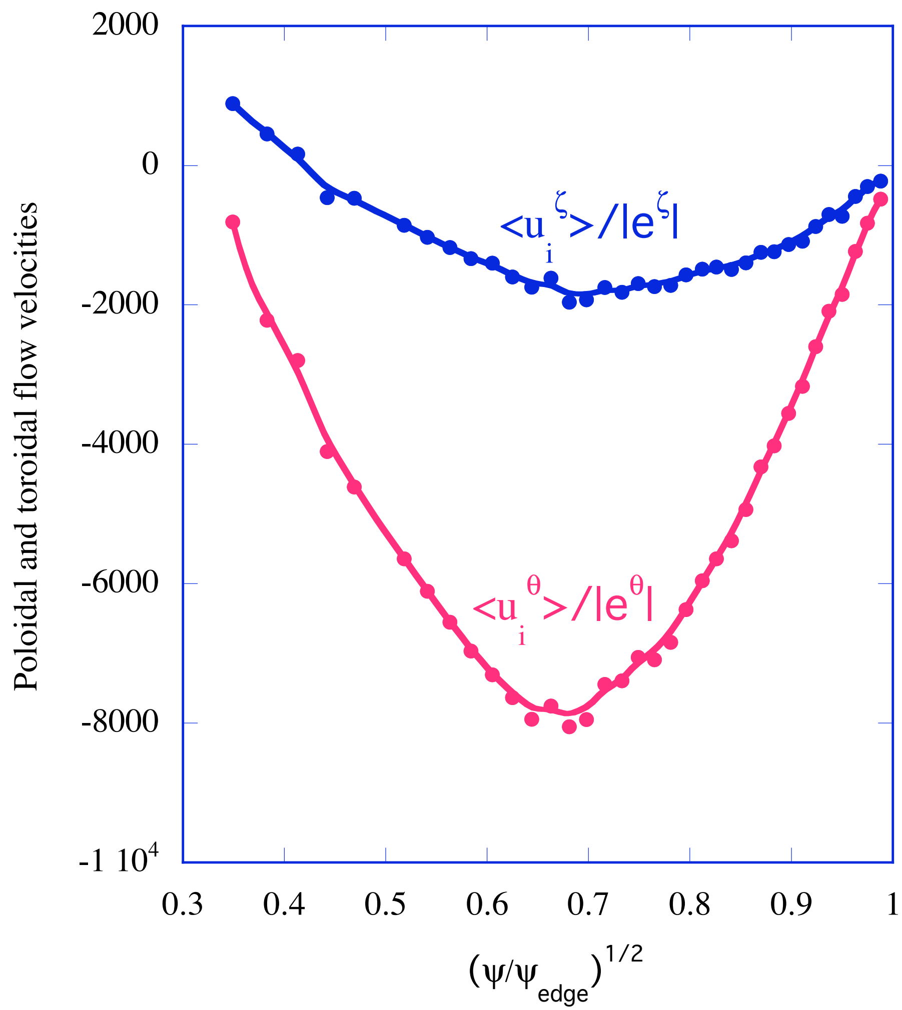

QPS ECH regime indicates a single electron root for $T_e(0) < 1.8$ keV and possibilities for bifurcated roots for $T_e(0) > 1.8$ keV

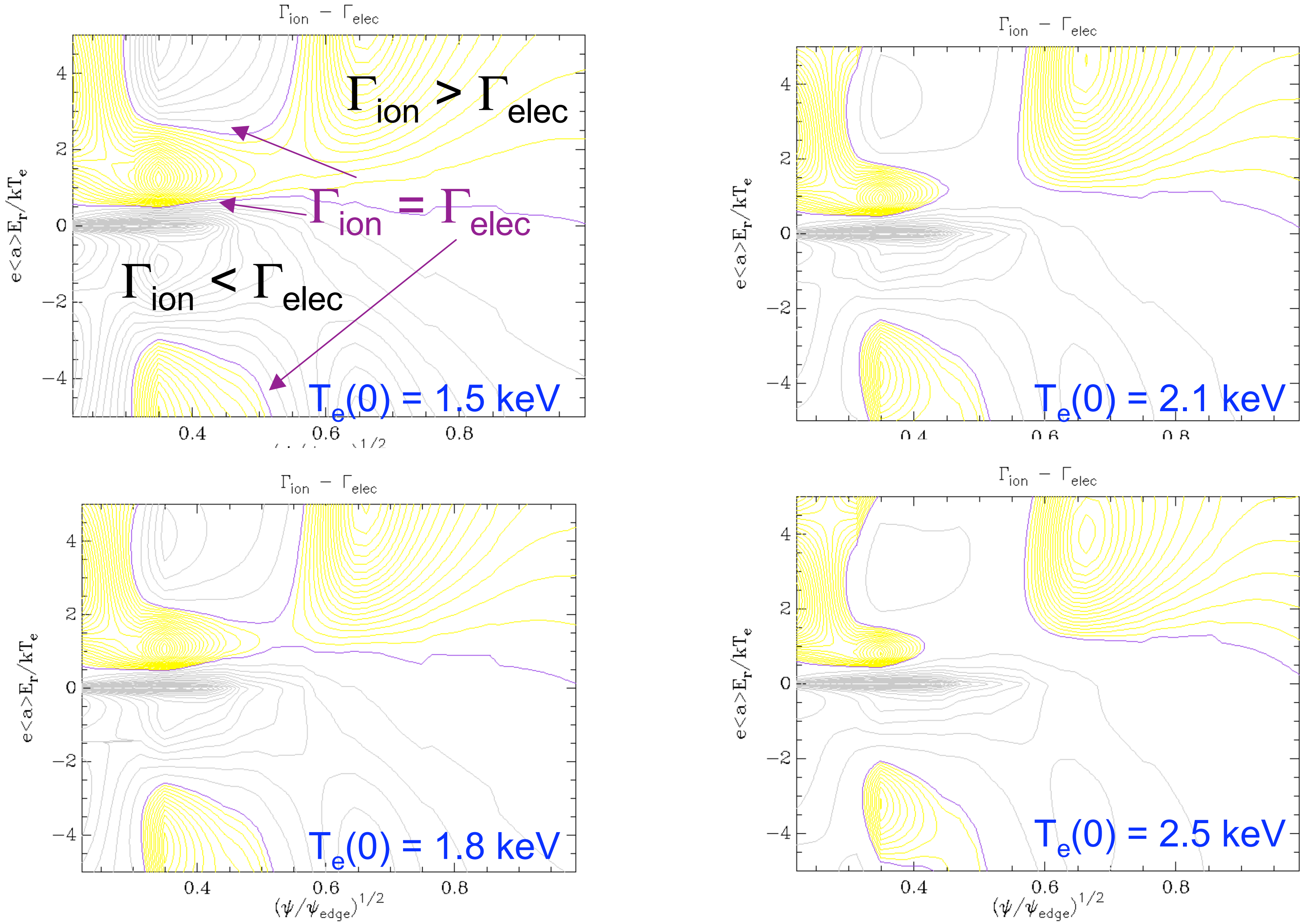

QPS - ECH regime

electric field and flow velocities

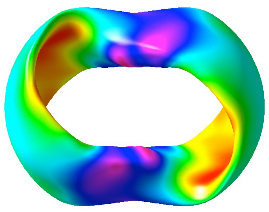

$n(0) = 2 \times 10^{19}$ m^{-3}, $T_e(0) = 1.8$ keV, $T_i(0) = 0.2$ keV

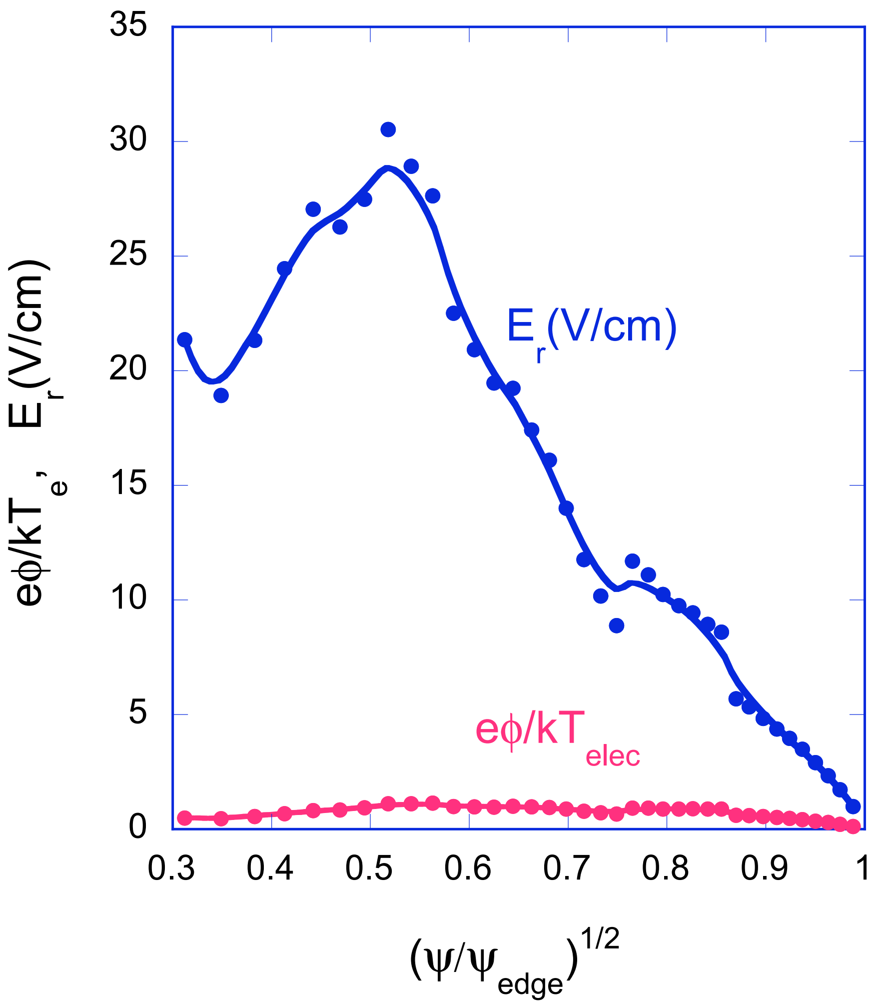

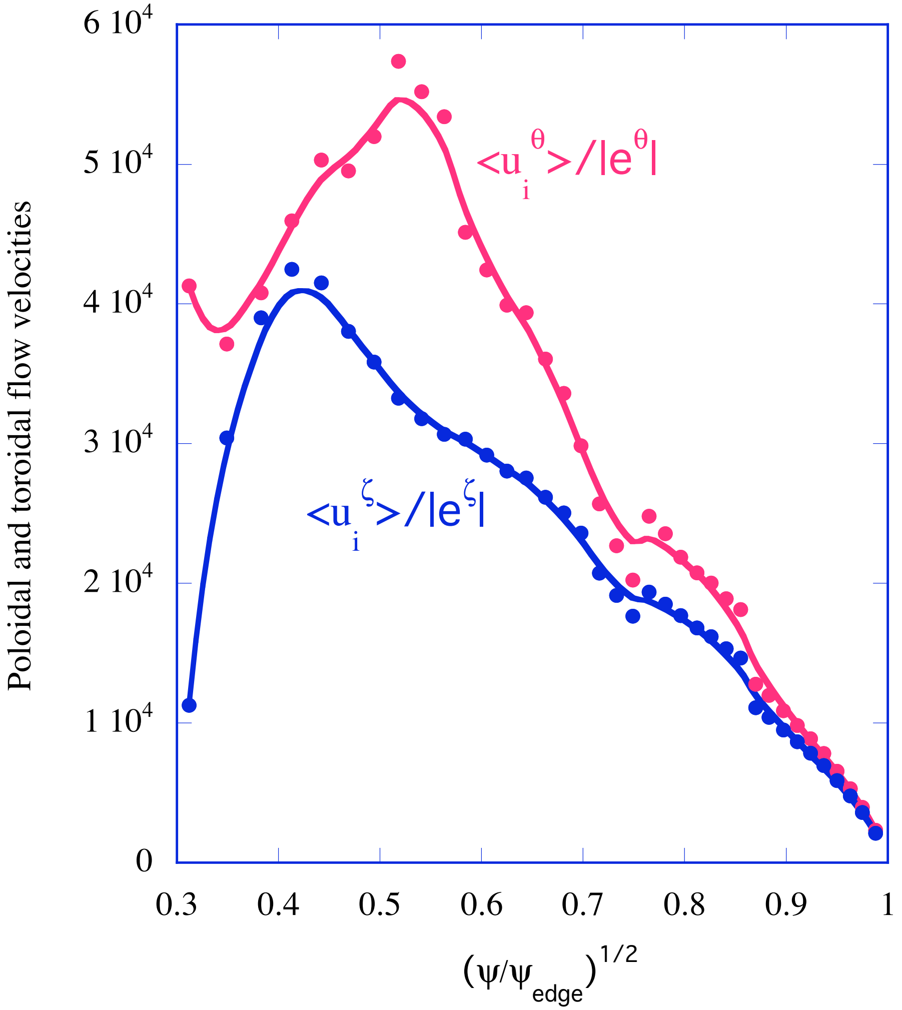

NCSX ICH regime has an ion root over the full radius

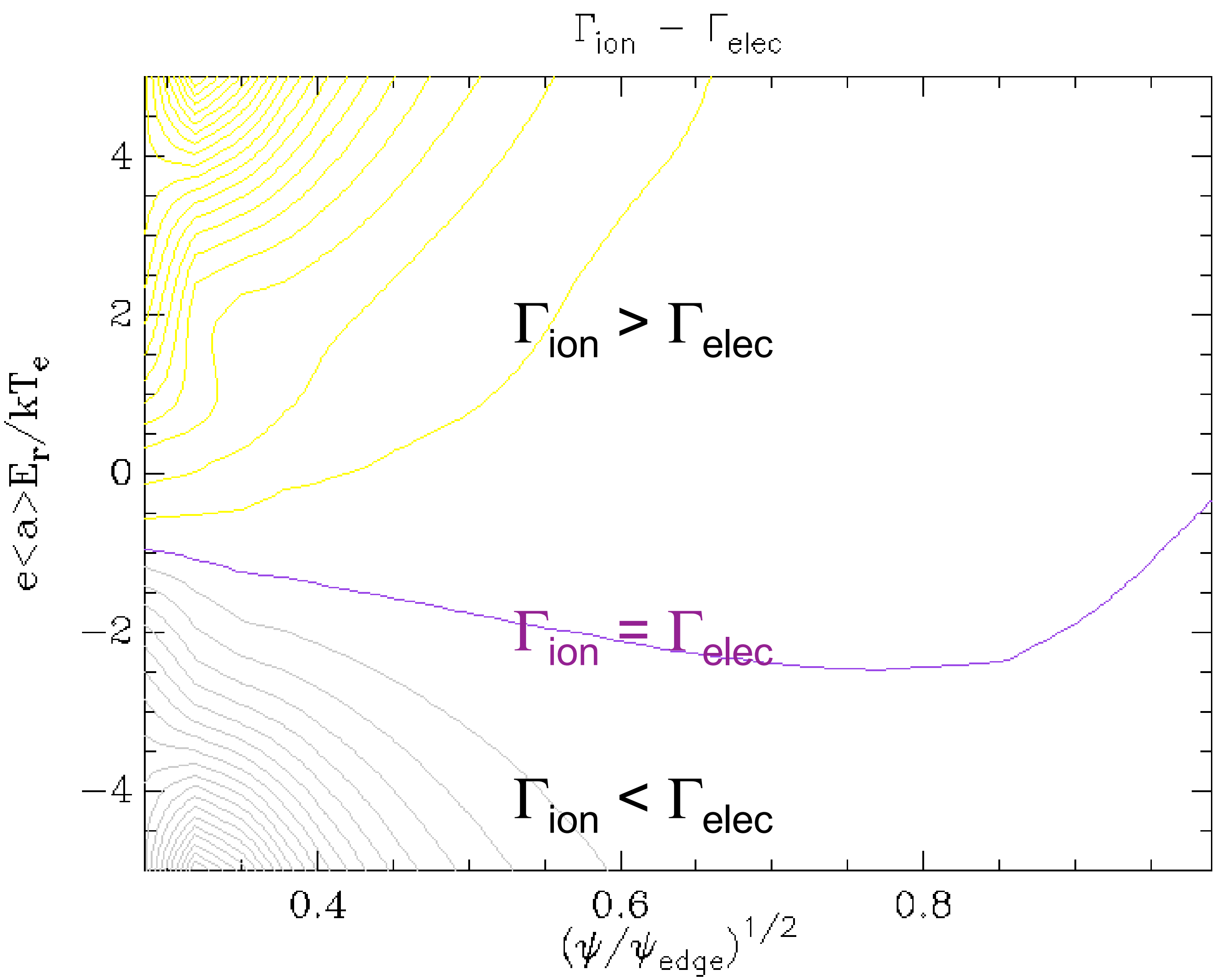

NCSX-ICH

electric field and flow velocities

Toroidal flow dominant in center, poloidal flow at edge

$n(0) = 8.3 \times 10^{19}\ m^{-3}$, $T_e(0) = 0.53$ keV, $T_i(0) = 0.38$ keV

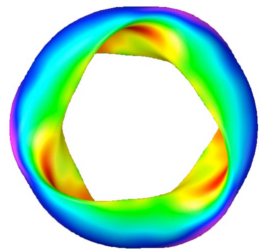

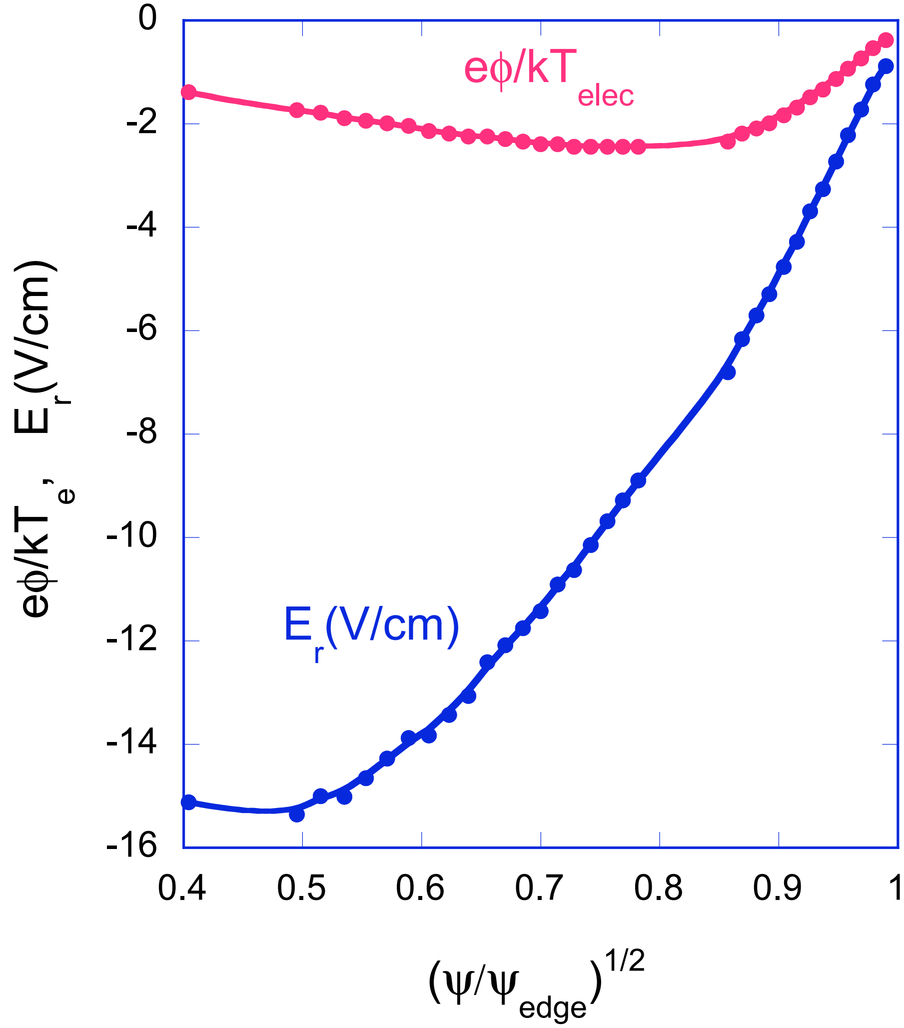

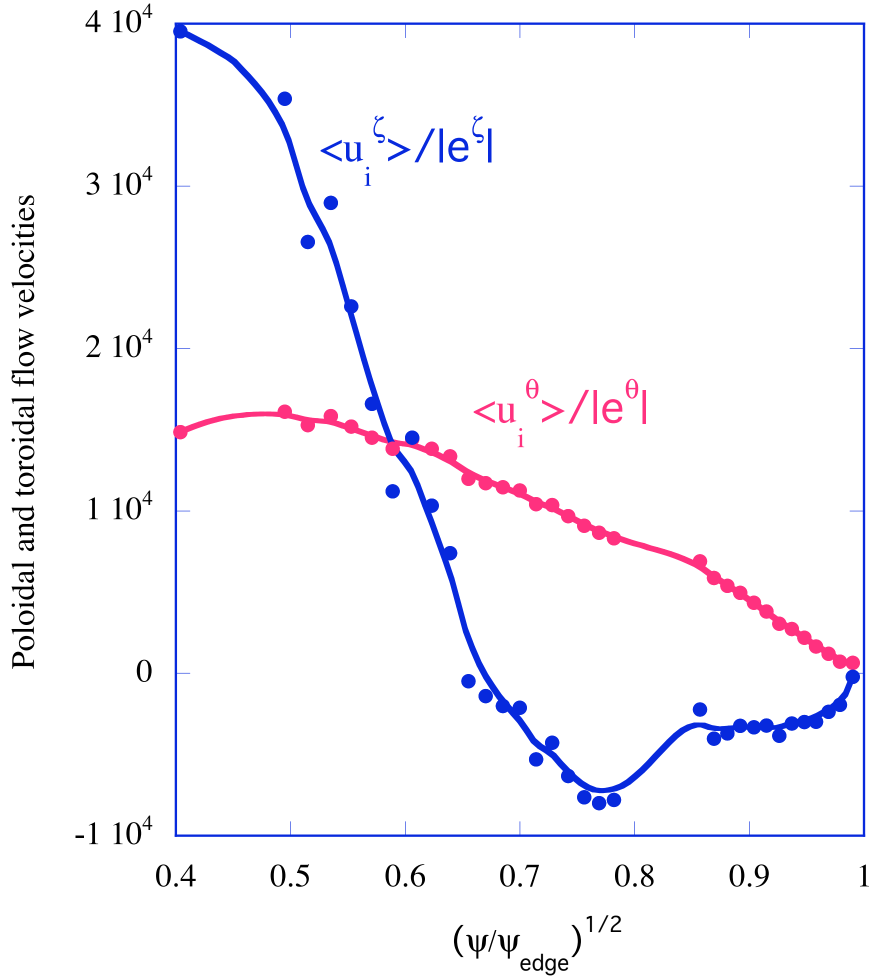

HSX ICH regime has an ion root over the full radius

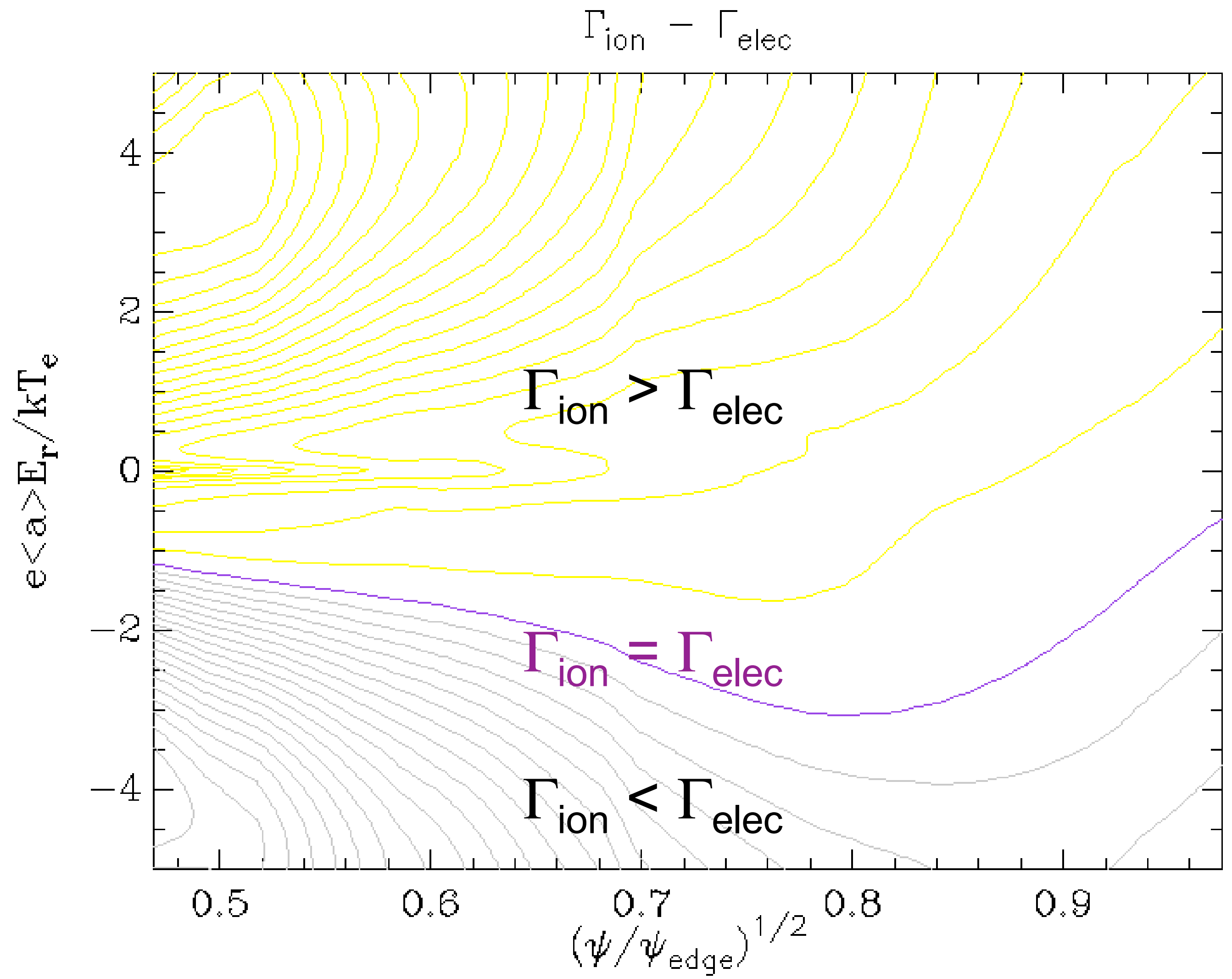

HSX - ICH

electric field and flow velocities

Flow follows helical |B| contours - mostly toroidal

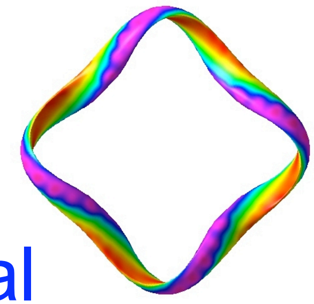

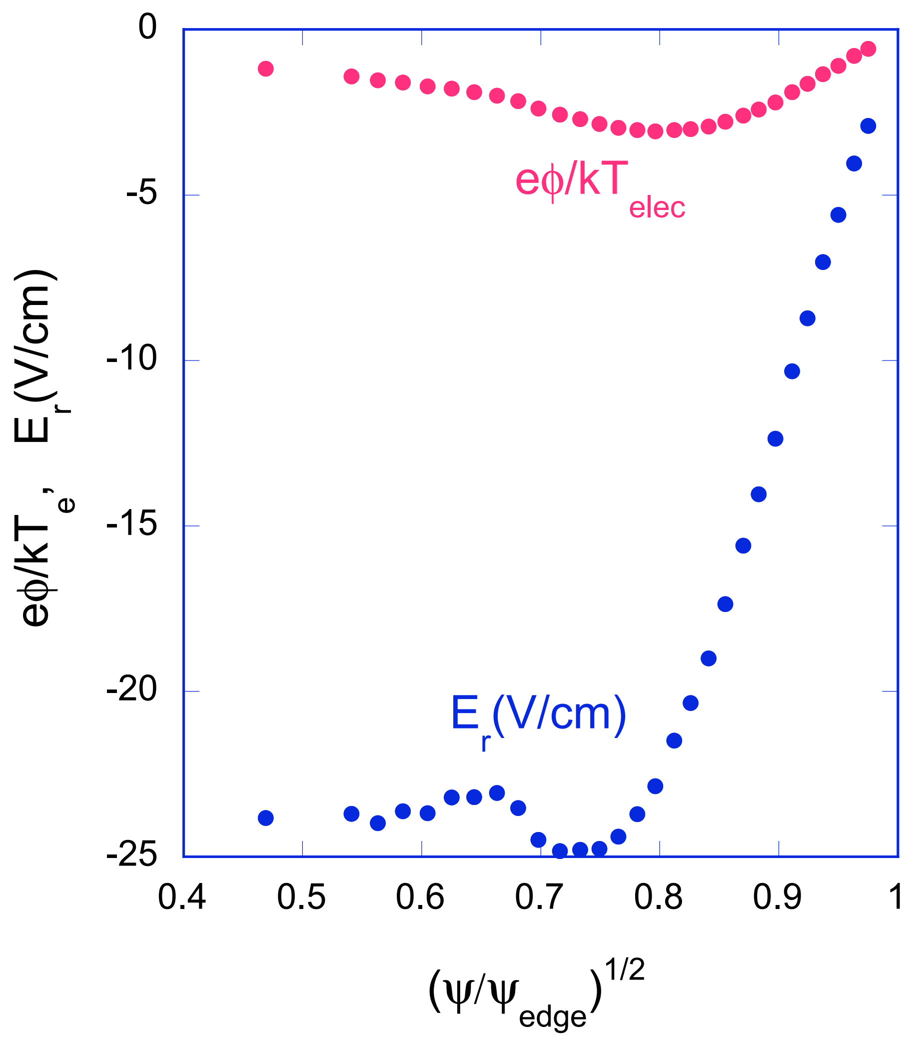

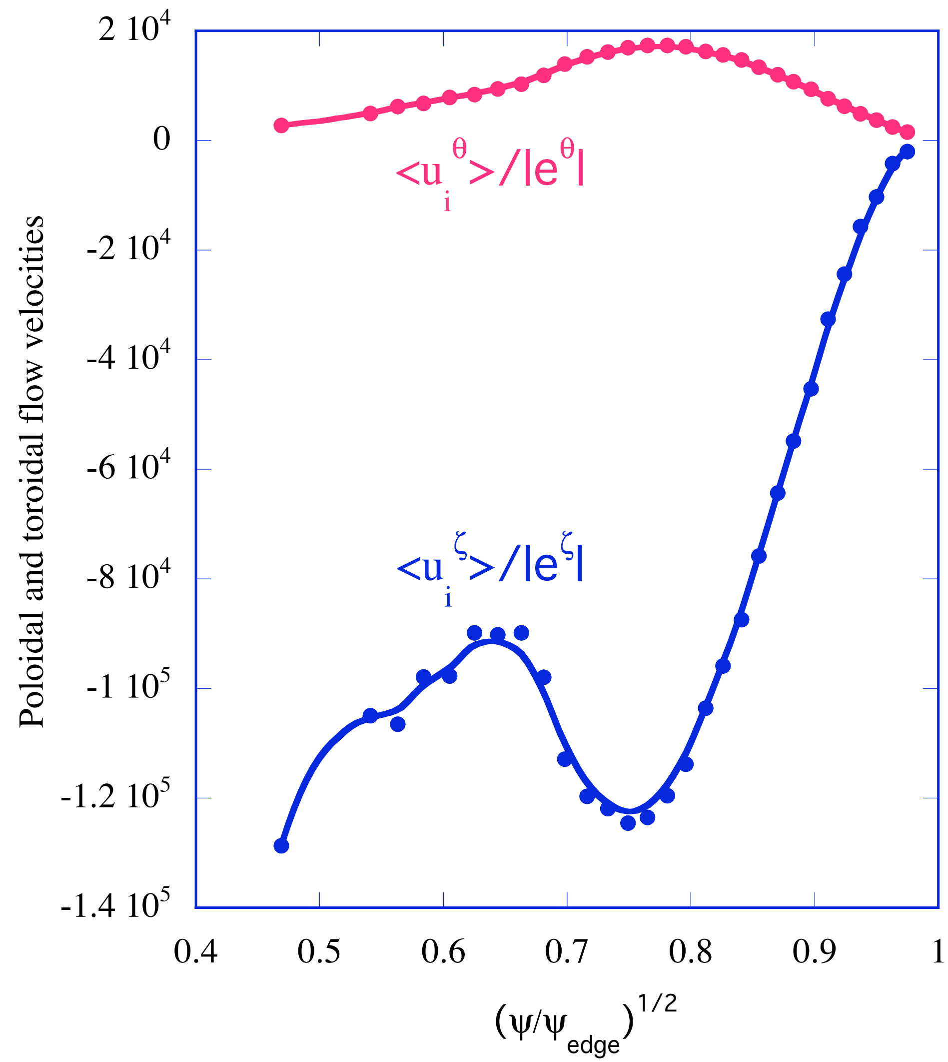

HSX ECH regime has an electron root over the full radius along with an ion root and a secondary electron root

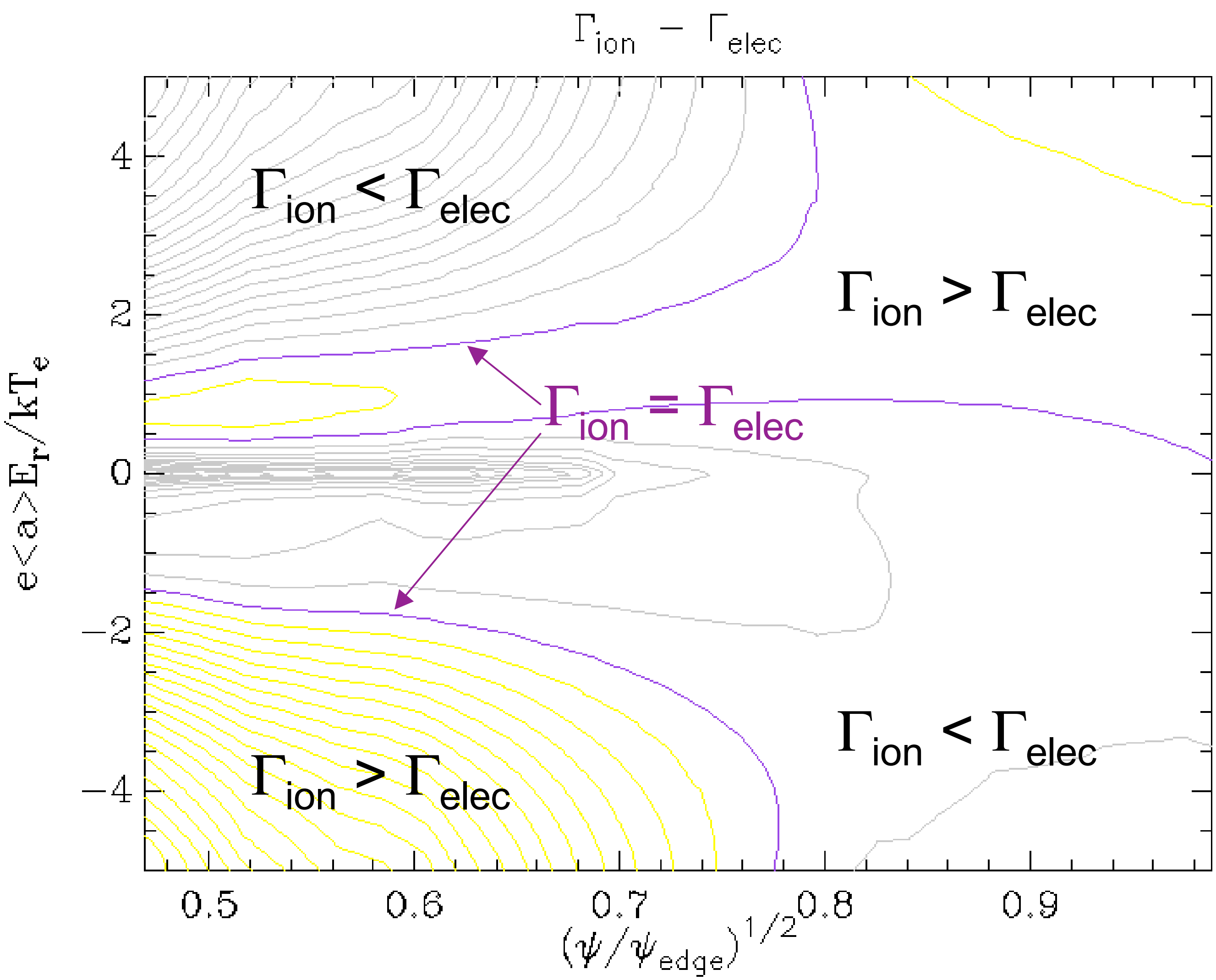

HSX - ECH

electric field and flow velocities

Flow follows helical |B| contours - mostly toroidal

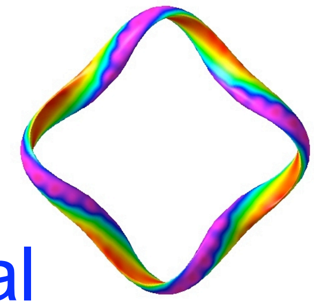

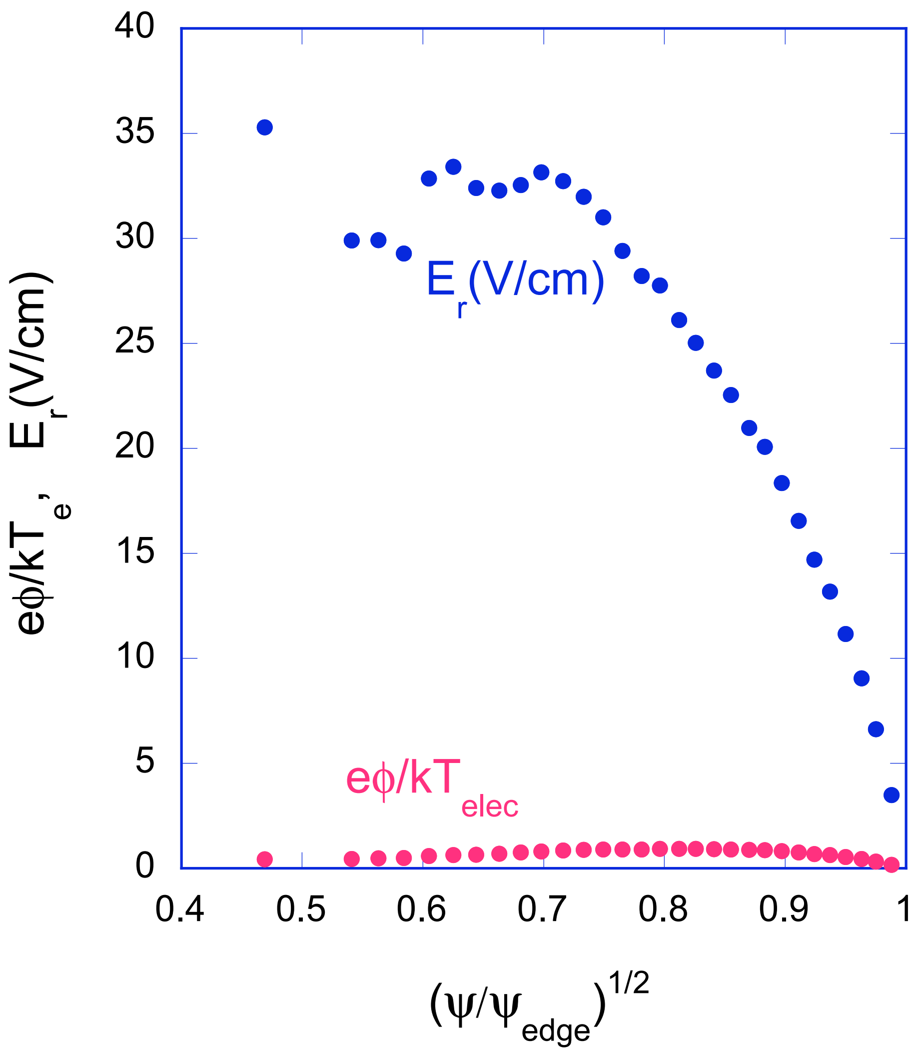

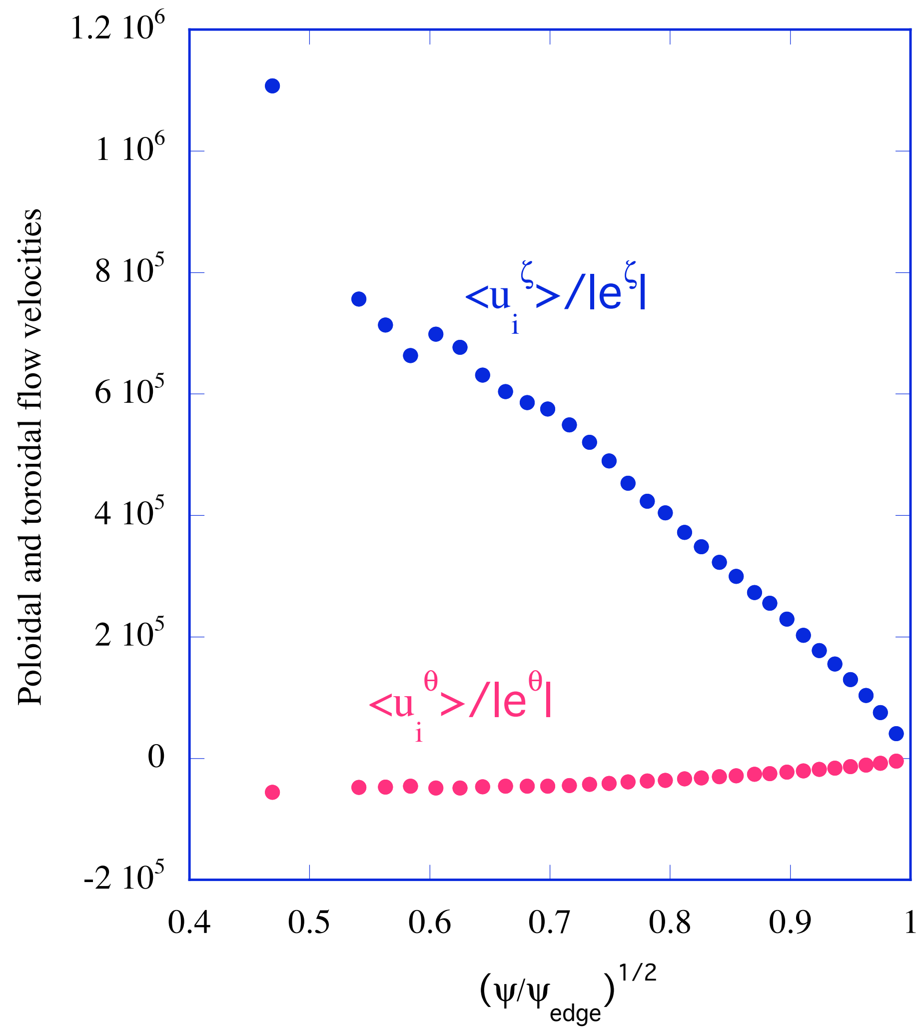

QPS offers substantial flexibility through 9 independently variable coil currents

QPS

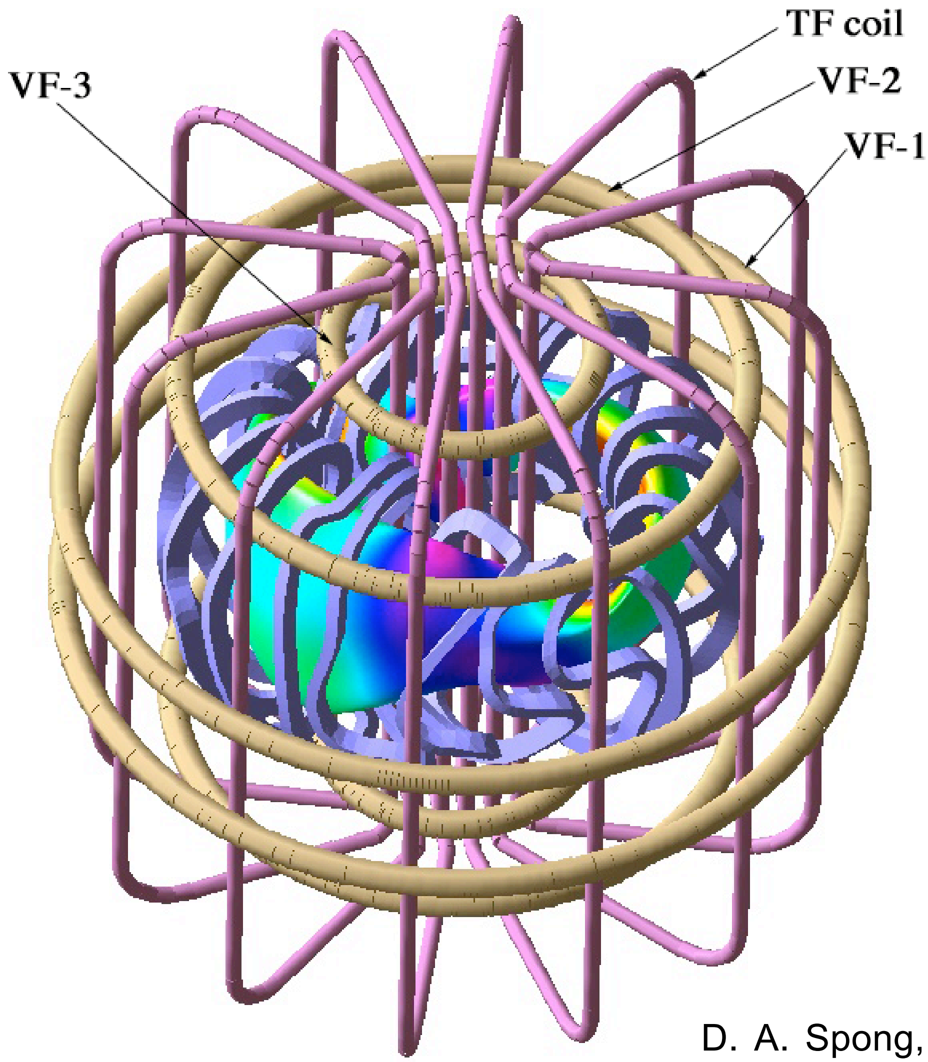

- Flexibility is a significant advantage offered by stellarator experiments
- Flexibility will aid scientific understanding in:
  - Flux surface fragility/island avoidance
  - Neoclassical vs. anomalous transport
  - Transport barrier formation
  - Plasma flow dynamics
  - MHD stability
- QPS offers flexibility through:
  - 5 individually powered modular coil groups
  - 3 vertical field coil
  - toroidal field coil set
  - Ohmic solenoid
    - Variable ratios of Ohmic/bootstrap current

D. A. Spong, D.J. Strickler, S.P. Hirshman, et al., QPS Transport Physics Flexibility Using Variable Coil Currents, Fusion Science and Technology 46, 215 (July, 2004).

QPS can vary low collisionality levels by a factor of ~25 and QP symmetry by a factor of ~10

QPS

Low collsionality transport

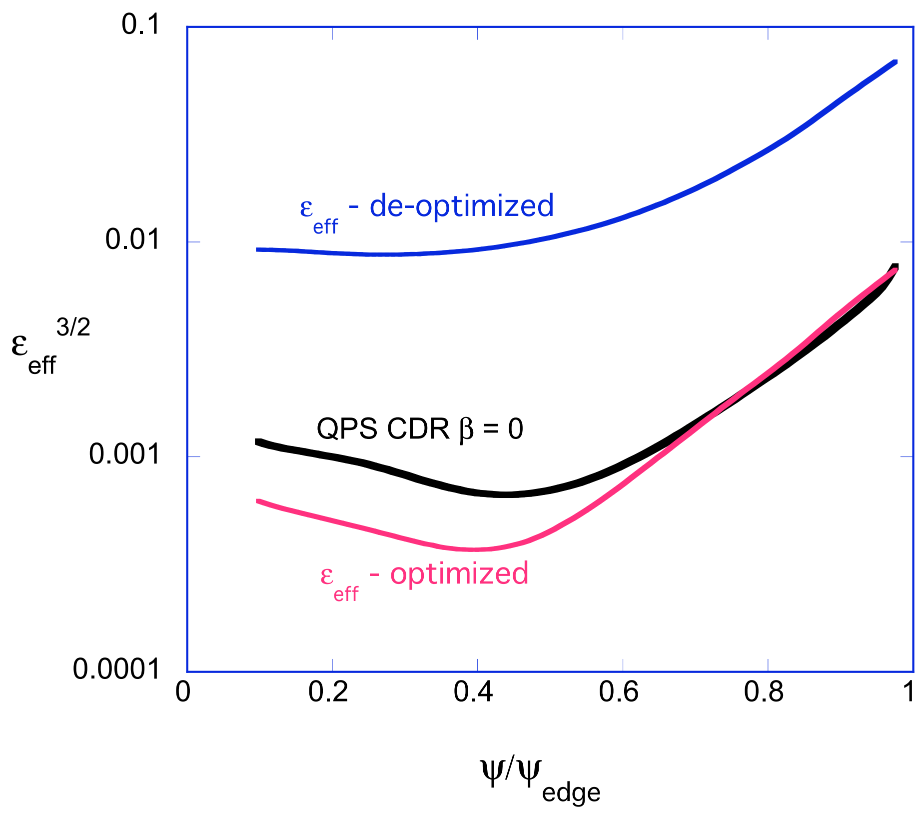

QP-symmetry

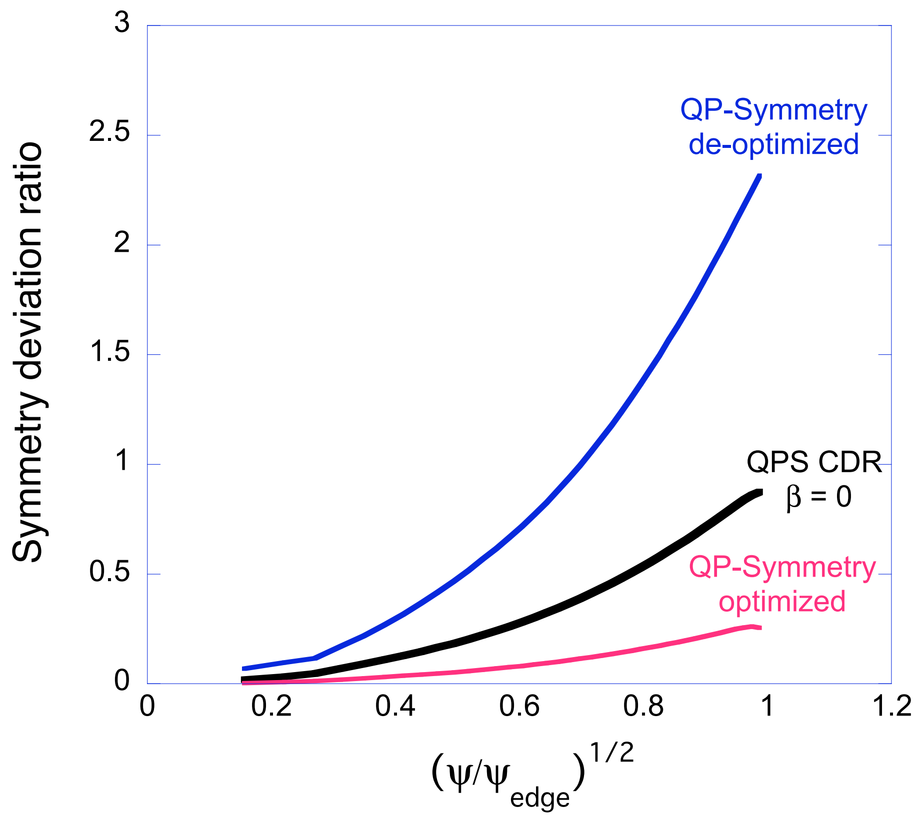

Collisional transport ($\nu \le$ plateau regime) shows a factor of ~25 variation. Poloidal viscosities show factor of 5-30 variation.

QPS

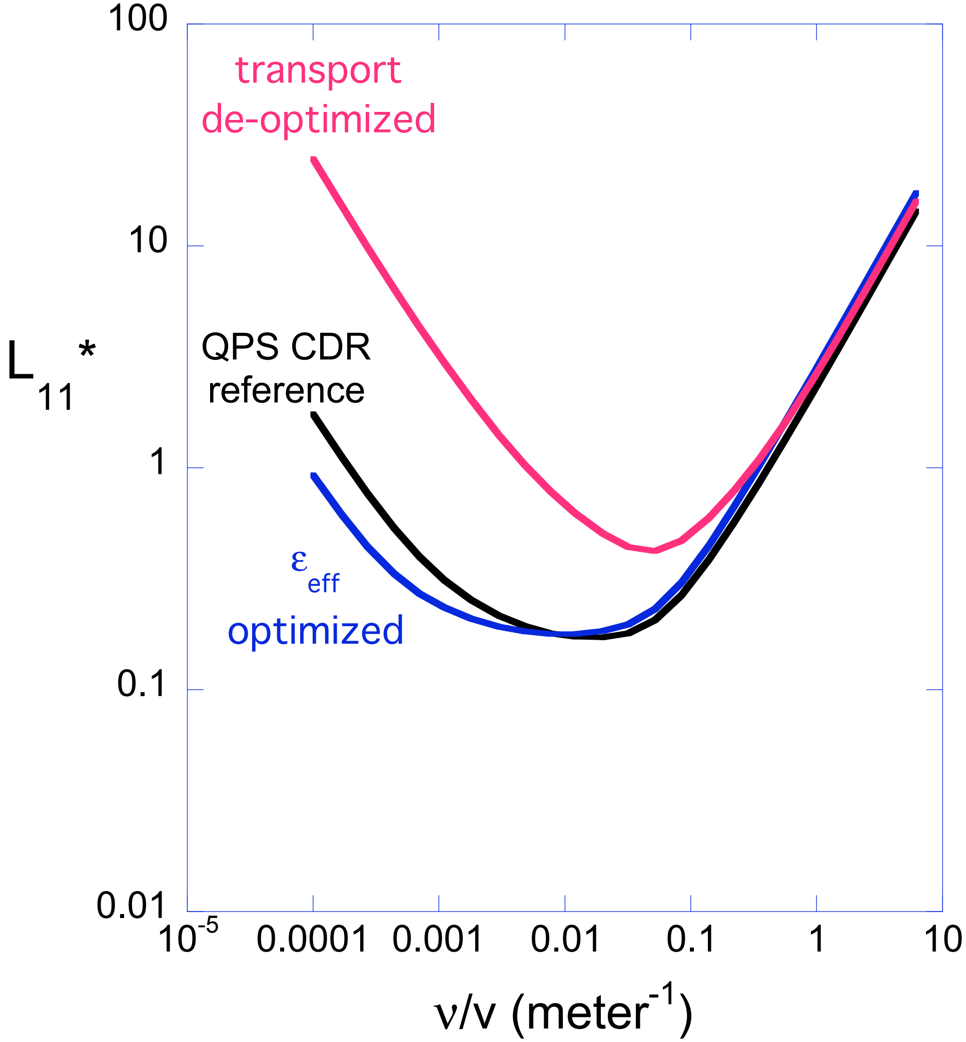

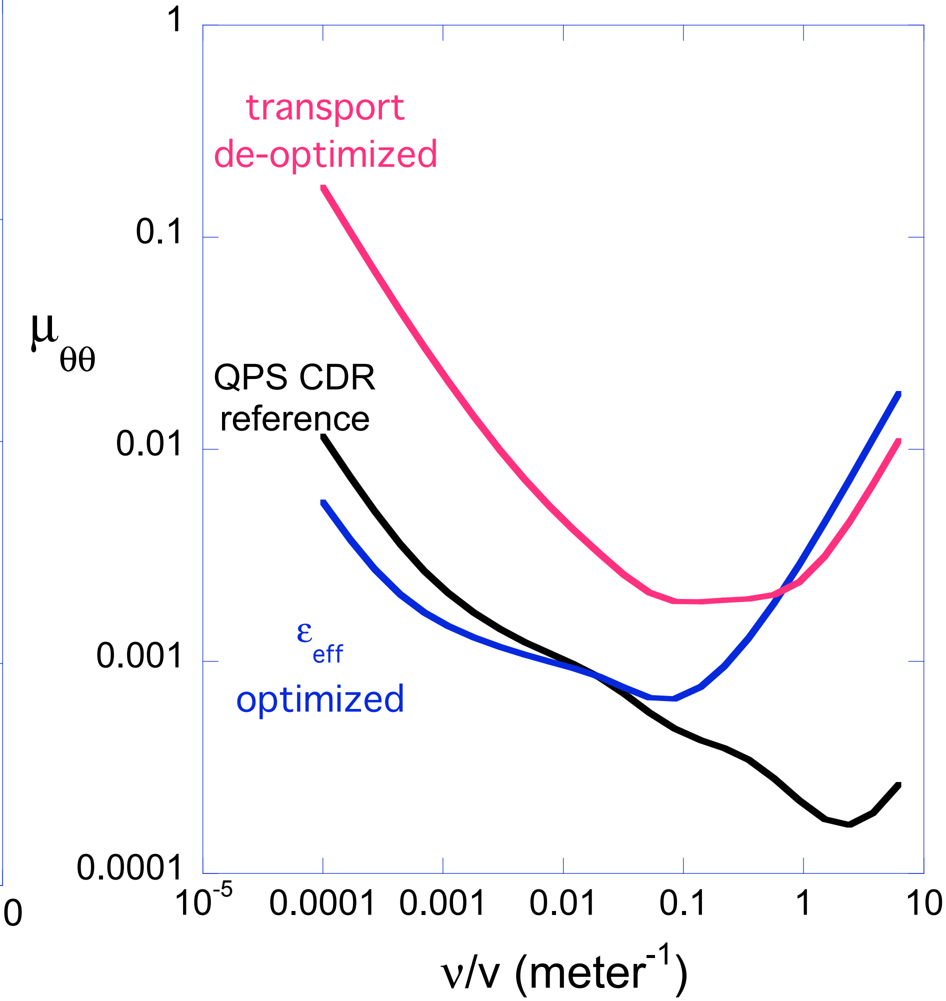

Conclusions

- A self-consistent ambipolar model has been developed for the calculation of flow profiles in stellarators
  - Parallel computation of DKES transport coefficient database
  - Extensions to low and high collisionality regimes as needed for energy integrations
  - Axisymmetric limit (i.e., $\Gamma_{ion} = \Gamma_{elec}$ at E_r = 0) verified
  - Ambipolar electric field solution
  - Predicted profiles of E_r, $\langle u^\theta \rangle$, and $\langle u^\zeta \rangle$
- Relative magnitudes of poloidal/toroidal flows in quasi–symmetric stellarators is influenced by the structure of |B|
  - QPS: poloidal flows dominate over toroidal flows
  - NCSX: toroidal flows dominate in the center, poloidal flows at the edge
  - HSX: toroidal flows seem to dominate due to 1:4 pitch of constant |B| variation
- Flexibility
  - QPS: factor of 10 variation in viscosity through coil current variations

Future topics in development of the stellarator moments method

- – Continued refinement of transport coefficient calculation and connection formulas
- – Parallelization of DKES over electric field parameter
  - • Will speed up turn-around on different configurations
- – Multi-ion species
  - • Impurity flow velocities
  - • Impurity accumulation studies
- – flow damping from neutrals
- – Study the multiple electric field roots and their stability
- – Bootstrap current evaluation/benchmark
  - –DKES/BOOTSJ/NEO/G_{BS}/Monte Carlo
  - – Electric field dependence needed
- – External flow drive (bias electrodes, RF flow drive, beams)
- – Extension of Monte Carlo methods to viscosities
- – Develop methods for non-local transport

δf Bootstrap Current Calculation

[uses method of A. Boozer and M. Sasinowski, Phys. Plasmas **2** (1995) 610]

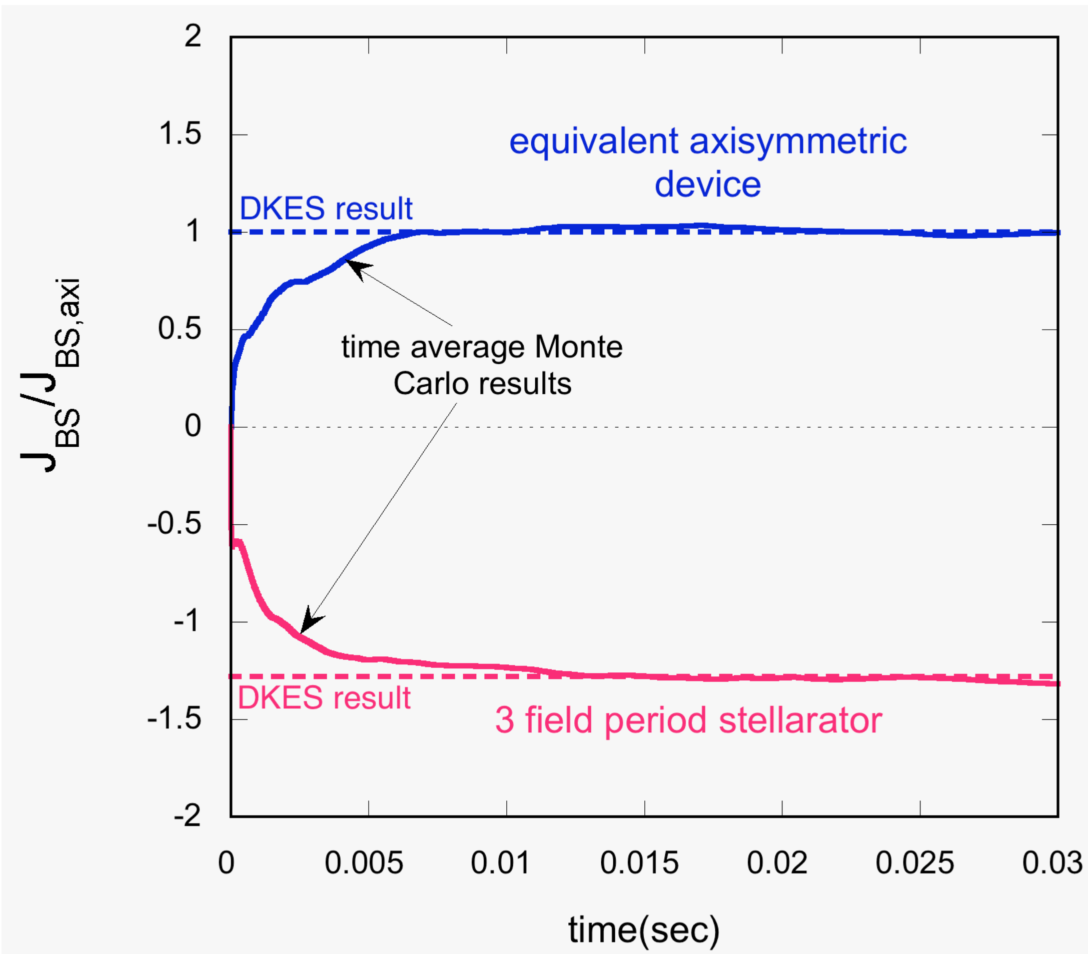

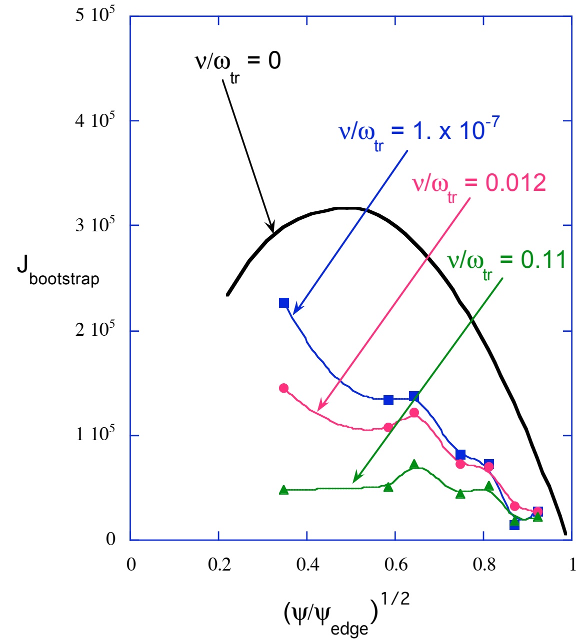

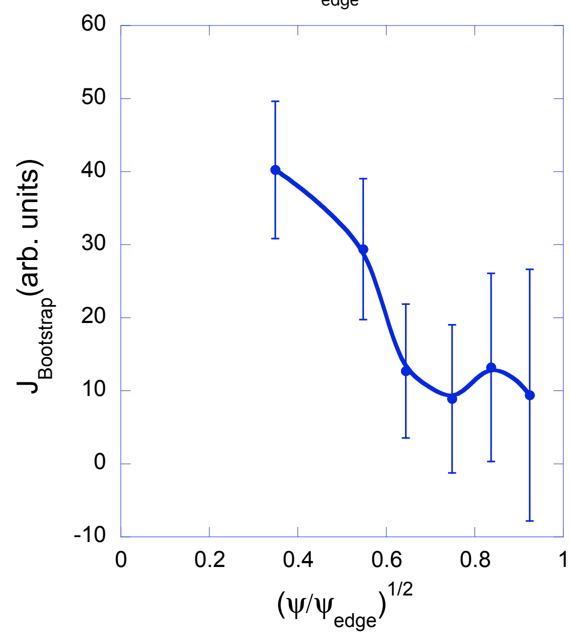

Stellarator transport: looking beyond the Fick's law paradigm

A. E. Fick, Annalen der Physik, 170, pg. 59-87 (1855).

$$\Gamma = -D\frac{\partial n}{\partial x}, \qquad \frac{\partial n}{\partial t} = D\frac{\partial^2 n}{\partial x^2}$$

Implies: $(x - \langle x \rangle)^2 \propto t$

Displacement vs. time of 10^4 ion orbits at
$n(0) = 8 \times 10^{19}\ m^{-3}$, $T_e(0) = T_i(0) = 500eV$, $E_r = 0$

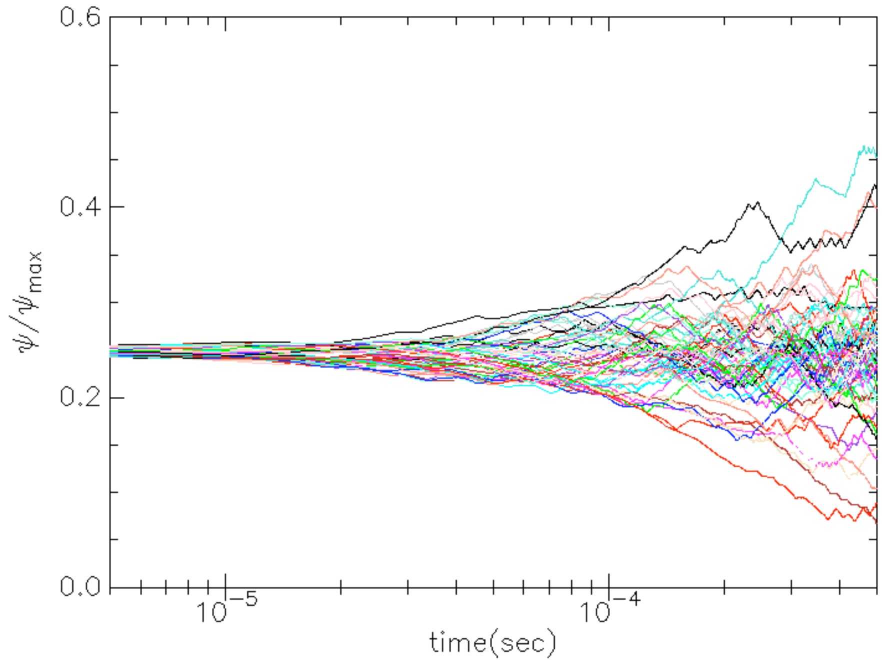

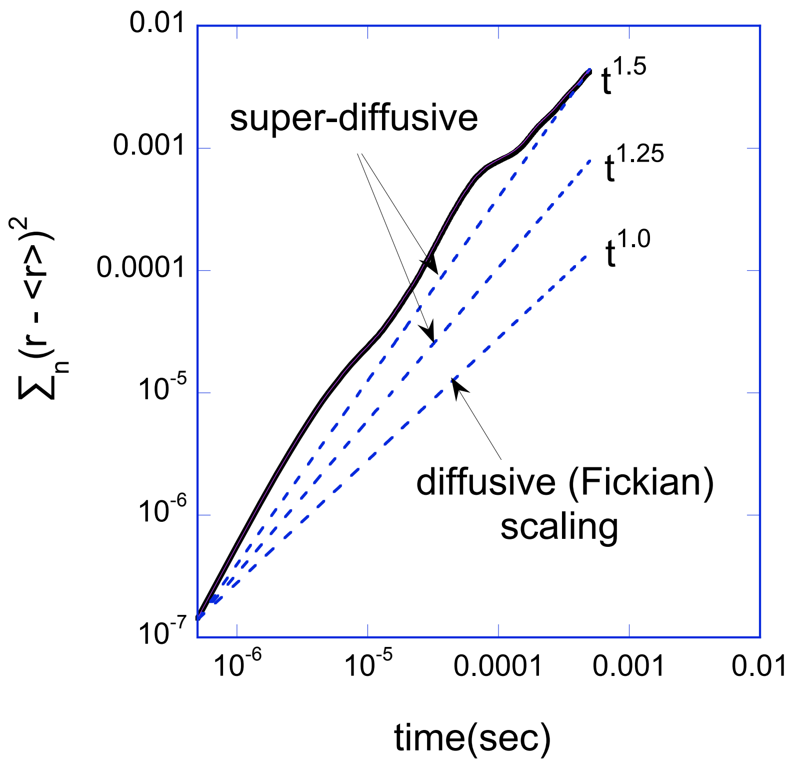

Fractional derivative diffusion equations allow a natural generalization of Fick's law:

$$\frac{\partial n}{\partial t} = D\frac{\partial^2 n}{\partial x^2} \Longrightarrow \frac{\partial^\beta n}{\partial t^\beta} = D\frac{\partial^\alpha n}{\partial x^\alpha}$$

Riemann-Liouville definition of fractional derivative:

$$\frac{\partial^\alpha n}{\partial x^\alpha} = \frac{1}{\Gamma(2-\alpha)}\int_0^x (x-x')^{1-\alpha}\, n(x')\,dx'$$

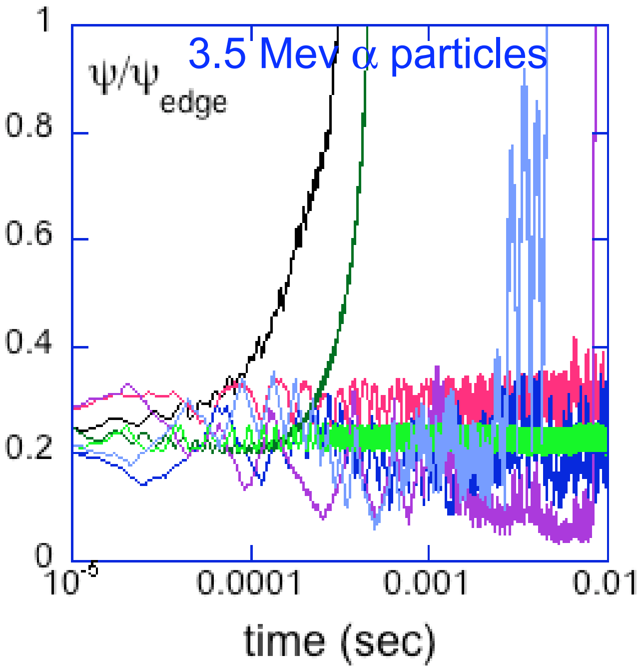

- Developed by Diego del-Castillo-Negrete and Ben Carreras to characterize plasma turbulence transport
- Fractional diffusion models can incorporate a variety of new effects:
  - Waiting time distributions
  - Anomalous (super/sub diffusive) transport
  - Asymmetrical transport
  - Intermittency
- Stellarator regimes
  - Low collisionality transport
  - Transport in the presence of islands
  - Transport in the presence of turbulence
  - Energetic particle transport